ハイリスク妊婦への情報提供実例集

C型肝炎

渡辺　博*,**　多田和美*,**　根岸正実**　大島教子**　稲葉憲之**

はじめに

C型肝炎は一本鎖RNAウイルスであるC型肝炎ウイルス(hepatitis C virus：HCV)の感染により発症する。HCVはウイルス性慢性肝炎の主要起因ウイルスである。妊婦がHCVに感染している場合には，時に肝機能異常を認めることはあるが，それ以外に自覚症状のないキャリアであることが多い。キャリア妊婦の問題は，母子感染により出生児にウイルスが持続感染するリスクがあることと，本人が将来慢性活動性肝炎・肝硬変・肝細胞癌を発症するリスクが20%前後あることである。

表　C型肝炎ウイルス検査を推奨されるのは(ウイルス肝炎研究財団)[1]

1. 平成4(1992)年以前に輸血(出産時を含む)を受けた
2. 大きな手術を受けた
3. 平成6(1994)年以前にフィブリノゲン製剤(フィブリン糊を含む)を投与された
4. 昭和63(1988)年以前に血液凝固製剤を投与された
5. 長期に血液透析を受けている
6. 平成4(1992)年以前に臓器移植を受けた
7. 薬物乱用者，入れ墨(タトゥー)をしている
8. ボディピアスを施している
9. その他(過去に健康診断等で肝機能検査の異常を指摘されているにもかかわらず，その後肝炎の検査をしていない)

頻度と検査法

我が国におけるHCVキャリアは2000年の推計では約150万人以上ともいわれている。過去にフィブリノゲン製剤や1992年以前の輸血を受けた場合など(表)には，HCV検査を受けることが推奨されている[1]。

HCVのスクリーニングはHCV抗体検査で行われ，厚生労働省は，妊婦健診において妊娠8週前後のHCV抗体検査は最低限必要な検査であるとの見解を通知しており(2007年1月16日)，現在では97%の妊婦がHCV抗体検査を受けている[2]。HCV抗体が陽性の場合HCV-RNA検査を行い，HCV感染が持続している(キャリア)か，現時点では感染していない既往感染者であるかの判定を行う。現在HCV-RNA検査は従来のHCV-RNA定性検査から，より高感度かつ広範囲にウイルス量が測定できるHCV-RNA定量検査(リアルタイムPCR法)に移行した。HCV-RNA定量検査では測定結果は「検出せず」(定性検査では陰性)と「検出」(定性検査では陽性)で示され，「検出」された場合の測定範囲は従来のHCV-RNA定性法・定量ハイレンジ法・定量オリジナル法での測定範囲を上回る15～69,000,000 IU/mLの広範囲に及ぶため，実数値ではなく対数値(1.2～7.8 LogIU/mL)で報告される。例えば治療のガイドラインのカットオフ値とされている100,000コピー/mL

わたなべ ひろし，ただ かずみ，ねぎし まさみ，おおしま きょうこ，いなば のりゆき
＊獨協医科大学病院総合周産期母子医療センター　＊＊獨協医科大学産科婦人科学教室
〒321-0293　栃木県下都賀郡壬生町北小林880

図　C型肝炎ウイルス(HCV)抗体陽性と診断された妊婦さんへ

今回の血液検査でC型肝炎ウイルス(HCV)抗体が陽性という結果が明らかとなりました。HCV抗体が陽性となるのは，C型肝炎を引き起こすウイルスに現在感染している場合と，過去に感染して現在ウイルスは排除されている場合です。我が国では0.3～0.8%の妊婦さんがHCV抗体陽性と診断されますが，そのうち70%の方は現在ウイルスが感染しており(キャリア状態)，残りの30%の方は過去の感染であるという調査結果があります。そのどちらであるかを区別するために，これからHCV-RNA定量検査という精密検査と肝機能検査(AST, ALTなど)を行います。

その結果で，

(1)HCV-RNA定量検査が陰性(検出せず)の場合

HCV-RNAが陰性(検出せず)であれば，現在C型肝炎ウイルスは体の中には存在しないと判定されます。したがって今回の妊娠でC型肝炎のウイルスがお子さんに感染することはありませんので，特別な対応をする必要はありません。念のため，お母さんからの抗体が消失する1歳6カ月以降にお子さんのHCV抗体を検査して，陰性であることを確認することが勧められています。

(2)HCV-RNA定量検査が陽性(検出)の場合

HCV-RNAが陽性(検出)と判定された場合，現在もウイルスに感染しているキャリア状態と診断されますので，今後肝臓の専門医を受診していただき，妊娠中・出産後の肝機能検査や内科的な対応を行うことが必要です。また出産時お子さんにC型肝炎ウイルスが感染する母子感染の可能性がありますが，その頻度は約10%です。特にお母さんの血中ウイルス量が多いほど，お子さんに感染する可能性が高いことが判明しています。ただしお子さんに感染した場合でも，約30%のお子さんは3歳頃までに自然に血中のC型肝炎ウイルスが排除されることも明らかとなっています。

○母子感染の予防法

我が国の調査では，妊婦さんのHCV-RNAが陽性(検出)の場合，陣痛が始まる前に予定帝王切開で出産すると，明らかに母子感染率が低いと報告されています。ただしウイルス量が多い場合でも経腟分娩で感染しないことが少なくありません。現状では帝王切開の危険性と感染した児の自然経過を考慮して，ご家族とともに分娩様式を決定することが勧められています。また母乳を通じてC型肝炎ウイルスがお子さんに感染することはありませんので，母乳で哺育されることには全く問題はありません。

○お子さんの検査と治療

お母さんがHCV-RNA陽性(検出)であった場合，出生後3～4カ月後に肝機能とHCV-RNAを検査します。その結果HCV-RNAが陽性であれば，3歳頃まで半年ごとにHCV抗体も含めて検査を行うことが勧められます。約30%のお子さんはHCV-RNAが陰性化してHCV抗体も陰性となりますが，その場合は治療は不要です。3歳の時点でHCV-RNAが陽性の場合はインターフェロンによる治療も選択肢となりますが，小児科の専門医と相談されることをお勧めします。治療をすることにより約半数のお子さんはC型肝炎ウイルスが消失しますが，実際にC型肝炎ウイルスが肝硬変や肝臓癌を引き起こして問題となるのは数十年後ですので，今後新たな治療法が開発される可能性があります。

○お母さんの治療

妊娠中には治療を行うことはありません。分娩終了後に肝臓専門医と相談してインターフェロンやリバビリンという抗ウイルス薬で治療を行うことが可能です。ただしこれらの薬は流産の原因となったり胎児に先天異常を起こすことがありますので，治療中は妊娠しないように注意してください。

は，約100 KIU/mLであるが，新しいHCV-RNA定量法では5 LogIU/mLと表現される。

妊婦におけるHCV抗体陽性率は0.3～0.8%であり，抗体陽性者の70%にHCV-RNAが検出される。したがってHCV抗体陽性だけでキャリア妊婦と即断してはいけない。HCV-RNAが検出されたことを確認した後，妊婦本人にその事実と，母子感染率，感染要因，児の経過，治療，妊婦自身の管理について，平易な言葉で，理解度を確認しながら説明する。HCV-RNA検出妊婦からの出生児の約10%が母子感染によりHCVキャリアとなるが，3歳頃までに30%の児ではウイルスが自然

に排除されて脱キャリア化することが判明した[3]。我が国の出生数から類推すると，毎年200～400名前後の新生児が母子感染している計算になり，輸血や血液製剤による感染がほぼ防止できるようになり，15歳未満の年代ではHCVキャリアは極めて少数(0.02～0.05%程度)[1]となった現在，母子感染を防止する対策が急務である。

妊娠中の対応

妊娠初期の検査でHCV抗体が陽性と判明した場合には，肝機能検査とともにHCV-RNA定量検査を行う。HCV-RNAの結果が「検出せず」であれば既往感染と判定され，今回の妊娠で母子感染が成立する懸念はなくなる。HCV-RNAが検出された場合はHCVキャリアと診断されるが，その結果は直接妊婦本人に通知し説明する。配偶者や家族に伝えるかどうかは，血液を介した感染のリスクや母子感染の頻度などを本人に説明した上で，妊婦本人の意志を尊重して決定する。診断結果を家族に説明した後に，家族が希望すればHCV抗体検査を実施する。HCV-RNAが検出された妊婦は，内科医，特に肝臓専門医に紹介して，妊娠中はもとより出産後の適切な診断や指導，治療を行うための管理を依頼する。それにより将来の治療必要性・治療方法・治療時期などの判断が円滑に行われることが期待される。またHCVキャリアという理由で，妊娠中の日常生活に制限を加える必要はない。

出産時の対応

HCV母子感染のリスクファクターとしてHIVの重複感染(3～4倍上昇)と，血中HCV-RNA量の高値(10^6コピー/mL=6.0 LogIU/mL以上)があげられている。我が国ではHIVの重複感染は極めて稀である。分娩様式では予定帝王切開で感染率が有意に低くなること，陣痛の発来や経腟分娩，産道での母体血への曝露が感染率を上昇させることが報告されている[4]。ただし血中HCV-RNAが高値であることを帝王切開の適応とすることに関しては，現時点では国内外でも統一された見解はなく，さまざまな議論がある。母子感染率が10%前後であること，感染児の自然経過(約30%が脱キャリア化)と小児期の治療成績(約50%がインターフェロン療法により治癒)，キャリア化した小児のほとんどは成人になるまでC型慢性肝炎に進行することはないため，今後の治療法の進歩により長期予後の改善が期待できること，などが必ずしも帝王切開を推奨しない理由としてあげられている。また帝王切開が母体に与えるリスクと，一度帝王切開で出産すると，次回以降の出産時にも帝王切開が選択されやすいこと，帝王切開後の妊娠では癒着胎盤などの母体合併症のリスクが若干増加することなども懸念されている。

ただし，HCV-RNAが高値の妊婦では，上記の帝王切開が母子に与えるリスク，HCVの母子感染率，感染児の自然経過，治療成績など，我が国で今日まで集積された情報を提示して，妊婦とその家族の意向を尊重して対応すべきとの意見もある。

出生児への対応

母乳からHCV-RNAが検出された報告はあるが，母乳哺育は母子感染率を増加させないと結論されており，HIV感染や乳頭からの出血などがなければ，原則として母乳哺育を推奨する。出生児のHCV抗体は母親からの移行抗体の影響で，生後12カ月過ぎまで陽性が続くこともあり，この時期までは母子感染の指標とならない。

HCV抗体陽性でHCV-RNA「検出せず」の母親からの出生児では，これまで母子感染は報告されていない[3]が，生後18カ月以降にHCV抗体を検査して陰性であることを確認する。

臍帯血や出生後1カ月以内のHCV-RNAの結果は，その後の経過と必ずしも一致しないため，

その解釈は慎重であるべきとされている。生後3～4カ月の時点でHCV-RNAの測定を開始して検出された場合，再度の検査で確認する。その結果「検出」が間違いなければ，生後6カ月以降半年ごとに肝機能検査(ALT，AST)とHCV-RNA，HCV抗体測定を実施して，持続感染の有無を確認する。半年以上の間隔で2回以上陽性(検出)を母子感染と定義した厚生労働省研究班の報告では，HCV-RNA陽性妊婦330名から34名(10.3%)に母子感染が成立していた[5]。生後3～4カ月でHCV-RNAが陰性(検出せず)の場合には，生後6カ月，12カ月の時点でHCV-RNAを検査して陰性(検出せず)を確認する。できれば生後18カ月以降にHCV抗体陰性化を確認して母子感染のフォローを中止する。母子感染例の30%は3歳頃までに血中HCV-RNAが消失するため，HCV感染児に対する治療は3歳以降とする。3歳以降もHCV感染が持続している小児に対してはAST，ALTの経過，HCV-RNA量，HCV genotypeなどの所見から，小児の肝臓専門医がインターフェロン療法などの適応を判断することになる。また感染児であっても保育園その他での集団生活を含め，児の日常生活に制限を加える必要はない。

母親への対応

妊娠中に母親の治療を行うことは禁忌とされているが，インターフェロン治療中に妊娠して異常のない児を出産したという報告は散見される。通常は分娩終了後に肝臓専門医の総合的な判断を基に，インターフェロン療法や抗ウイルス薬であるリバビリンによる治療を行うかどうかを選択することになる。ただしこれらの薬は流産の原因となったり胎児に先天異常を起こすことがあるため，治療中は妊娠しないように指導する。当科で3回の妊娠・出産をいずれも経腟分娩で行い，HCV-RNA低値であった第1子の出産で母子感染が成立したが3歳までに陰性化，HCV-RNA高値であった第2子は母子感染成立せず，その後インターフェロン治療を行い，HCV-RNA陰性の状態で第3子を出生した妊婦を経験している[6]。

おわりに

C型肝炎ウイルスキャリアと診断された妊婦とその出生児に対する情報提供について紹介した。HCV-RNA定量検査が従来法からリアルタイムPCR法に移行しており，結果の解釈と説明に混乱をきたさないようにする必要がある。また本稿の内容は「産婦人科診療ガイドライン産科編2008」の「CQ607妊娠中にHCV抗体陽性が判明した場合は？」[7]に準じて記載した。HCVの診断法・治療法は急速に進んでおり，近い将来新たな知見や治療薬の開発により，HCV母子感染に関する管理指導指針が変更される可能性は高い。

文献

1) ウイルス肝炎研究財団：Q&A C型肝炎について (http://www.vhfj.or.jp/06.qanda/about_ctype.html)
2) 稲葉憲之，大島教子，林田志峯，他：産婦人科性感染症マニュアル10. 肝炎ウイルス．産と婦 **75**：1504–1510, 2008
3) 白木和夫，大戸 斉，稲葉憲之，他：C型肝炎ウイルスキャリア妊婦とその出生児の管理ならびに指導指針．日児誌 **109**：78–79, 2005
4) Hayashida A, Inaba N, Oshima K, et al：Re-evaluation of the true rate of hepatitis C virus mother-to-child transmission and its novel risk factors based on our two prospective studies. J Obstet Gynaecol Res **33**：417–422, 2007
5) 大戸 斉：C型肝炎ウイルス等の母子感染防止に関する研究　厚生労働省科学研究補助金．平成18年度総括・分担研究報告書，pp1–18, 2007
6) 渡辺 博，西川正能，根岸正実，他：C型肝炎ウイルスキャリアの妊娠．JIM **18**：238–240, 2008
7) 日本産科婦人科学会/日本産婦人科医会：CQ607妊娠中にHCV抗体陽性が判明した場合は？　産婦人科診療ガイドライン産科編2008，pp160–162, 2008

Postinfection passive transfer of KD-247 protects against simian/human immunodeficiency virus-induced CD4$^+$ T-cell loss in macaque lymphoid tissue

Toshio Murakami[a], Yasuyuki Eda[a], Tadashi Nakasone[b], Yasushi Ami[c], Kenji Someya[d], Naoto Yoshino[b], Masahiko Kaizu[b], Yasuyuki Izumi[b], Hajime Matsui[a], Katsuaki Shinohara[e], Naoki Yamamoto[b] and Mitsuo Honda[b]

Background: Preadministration of high-affinity humanized anti-HIV-1 mAb KD-247 by passive transfer provides sterile protection of monkeys from heterologous chimeric simian/human immunodeficiency virus infection.

Methods: Beginning 1 h, 1 day, or 1 week after simian/human immunodeficiency virus-C2/1 challenge (20 50% tissue culture infective dose), mature, male cynomolgus monkeys received multiple passive transfers of KD-247 (45 mg/kg) on a weekly basis for approximately 2 months. Concentrations and viral loads were measured in peripheral blood, and CD4$^+$ T-cell counts were examined in both peripheral blood and various lymphoid tissues.

Results: Pharmacokinetic examination revealed similar plasma maintenance levels ranging from 200 to 500 μg/ml of KD-247 in the three groups. One of the six monkeys given KD-247 could not maintain these concentrations, and elicitation of anti-KD-247 idiotype antibody was suggested. All monkeys given KD-247 exhibited striking postinfection protection against both CD4$^+$ T-cell loss in various lymphoid tissues and atrophic changes in organs compared with control group animals treated with normal human immunoglobulin G. The KD-247-treated groups were also partially protected against plasma viral load elevation in peripheral blood samples, although the complete protection previously reported with preadministration of this mAb was not achieved.

Conclusion: Postinfection passive transfer of humanized mAb KD-247 with strong neutralizing capacity against challenged virus simian/human immunodeficiency virus-C2/1 protected CD4$^+$ T cells in lymphoid organs.

© 2009 Wolters Kluwer Health | Lippincott Williams & Wilkins

AIDS 2009, **23**:1485–1494

Keywords: anti-V3 mAb, CD4$^+$ T cells, HIV-1, KD-247, lymphoid tissue, passive immunization, simian/human immunodeficiency virus

Introduction

Elicitation of virus-specific humoral immune responses, with their strong CD4$^+$ and CD8$^+$ T-cell immune responses, are critical to good control of HIV-1 [1,2]. Although recent vaccine candidates based on active immunization are intended to stimulate CD4$^+$ and CD8$^+$ T-cell responses, induction of broadly neutralizing

[a]The Chemo-Sero-Therapeutic Research Institute (Kaketsuken), Kyokushi, Kikuchi, Kumamoto, [b]AIDS Research Center, [c]Division of Experimental Animal Research, [d]Department of Virology III, and [e]Division of Biosafety Control, National Institute of Infectious Diseases, Shinjuku-ku, Tokyo, Japan.

Correspondence to Toshio Murakami, PhD, The Chemo-Sero-Therapeutic Research Institute (Kaketsuken), Kyokushi, Kikuchi, Kumamoto 869-1298, Japan.

Tel: +81 968 37 3172; fax: +81 968 37 3930; e-mail: murakami-tos@kaketsuken.or.jp

Received: 8 January 2009; revised: 7 April 2009; accepted: 18 May 2009.

DOI:10.1097/QAD.0b013e32832e5331

Copyright © Lippincott Williams & Wilkins. Unauthorized reproduction of this article is prohibited.

antibodies by active immunization has been limited to date [3,4]. In contrast, passive immunization with neutralizing antibody effectively induced sterilizing immunity by preventing the establishment of chronic infection. We and others have reported that chimpanzees can be protected against acute infection with the T-cell line-adapted strain HIV-1_{IIIB} by passive transfer of a mouse–human chimeric anti-HIV-1 V3 mAb [5]. Furthermore, we produced a high-affinity cross-neutralizing humanized mAb, KD-247, by sequential immunization with peptides derived from the V3 region of HIV-1 clade B primary isolates and found that KD-247 yields sterile protection of monkeys against the highly pathogenic simian/human immunodeficiency virus (SHIV) [6,7]. KD-247 is thus considered a promising new immunotherapeutic agent for HIV-1-infected patients [8].

It was demonstrated that intensive, short-term postinfection therapy with neutralizing immunoglobulin G (IgG) against simian immunodeficiency virus (SIV) can have long-term beneficial effects on disease in a pathogenic primate lentivirus model [9]. Passive transfer of neutralizing antibodies also conferred postinfection prophylaxis against pathogenic SHIVs in macaques [10,11]. Furthermore, passive immunization of pregnant or neonatal monkeys with combinations of mAbs has been reported to completely or partially neutralize SHIV in animal models of mother-to-child transmission of HIV [12,13]. However, whether neutralizing antibody plays a significant role in controlling established HIV infection is unclear. The current aim of antiretroviral therapy remains the maintenance of plasma HIV-1 RNA levels below the limit of detection [14]. In a clinical trial, three passively transferred mAbs, 2G12, 2F5, and 4E10, were shown to delay the rebound of HIV-1 after cessation of antiretroviral therapy; the delay was particularly pronounced in acutely infected individuals [15]. In this study, we evaluated the postinfection effect of KD-247 against $CD4^+$ T-cell loss and increased viral loads in the SHIV model.

Materials and methods

Preparation of KD-247

A high-affinity humanized mAb, KD-247 [Chemical Abstracts Service (CAS) Registry Number: 914257-21-9], was prepared as previously described [6]. Briefly, the mouse mAb C25 was elicited by immunization with six synthetic peptides derived from the V3 region of HIV-1 primary isolates. The complementary-determining regions and partial framework regions of C25 were transferred into the variable region of human IgG. Cells producing the humanized C25, KD-247, were expanded in large-scale culture, and the antibody was purified from the culture supernatants by ion exchange and affinity chromatography.

Pathogenic simian/human immunodeficiency virus challenge to monkeys and postinfection transfer of KD-247

All animals used in this study were mature, male cynomolgus monkeys (*Macaca fascicularis*) from the Tsukuba Primate Center, the National Institute of Infectious Diseases (NIID) (currently known as the Tsukuba Primate Research Center, National Institute of Biomedical Innovation), Japan. They were housed in accordance with the Guidelines for Animal Experimentation of the Japanese Association for Laboratory Animal Science, 1987, under the Japanese Law Concerning the Protection and Management of Animals, and were maintained in accordance with the guidelines set forth by the Institutional Animal Care and Use Committee of NIID, Japan.

The pathogenic chimeric SHIV-C2/1 is an SHIV-89.6 variant isolated by in-vivo passage in cynomolgus monkeys [16]. Cynomolgus monkeys injected intravenously with SHIV-C2/1 exhibited high levels of viremia and marked $CD4^+$ T-cell depletion within 2 weeks after challenge [16,17]. Six naive monkeys were intravenously inoculated with 20 50% tissue culture infective dose ($TCID_{50}$) of SHIV-C2/1 and were then given 45 mg/kg weight of KD-247 at 1 h (Cy-1 and Cy-2), 1 day (Cy-3 and Cy-4), or 1 week (Cy-5 and Cy-6) after viral challenge; a single preinfection administration of the mAb at this dosage had exhibited sterile protection against SHIV-C2/1 infection [7]. Two control monkeys (Cy-7 and Cy-8) received 45 mg/kg of purified human normal immunoglobulin (control IgG; Nihon Pharmaceutical, Tokyo, Japan) instead of KD-247 at 1 day after viral challenge. Additional multiple (seven or eight) administrations of the same concentrations of KD-247 or control IgG were given weekly from day 7 for a period of 2.5–3 months. Blood samples were drawn to examine the plasma concentrations of KD-247, SHIV RNA copy numbers, and $CD4^+$ T-cell counts. At approximately 11–13 weeks after viral challenge, necropsies were performed and histological examination and flow cytometric analyses of lymphoid organs were conducted. The schedules of KD-247 administration, blood drawing, and necropsy are shown in Fig. 1(a).

Plasma concentration of KD-247

KD-247 concentrations in macaque plasma were measured by ELISA. Ninety-six-well ELISA plates (MaxiSorp, Nunc A/S, Roskilde, Denmark) were coated with a KD-247-specific antigen, SP13 peptide (GPGRAFGPGRAFGP GRAFC). After blocking and washing, monkey plasma at appropriate dilutions was added and the plates incubated. KD-247 was diluted to concentrations ranging from 2.5 to 40 ng/ml and used as a reference. The wells were washed and then incubated with a detection antibody solution consisting of peroxidase-conjugated antihuman IgG mAb (Kaketsuken, in-house preparation). After final washes, peroxidase substrate was added and the reaction was

Copyright © Lippincott Williams & Wilkins. Unauthorized reproduction of this article is prohibited.

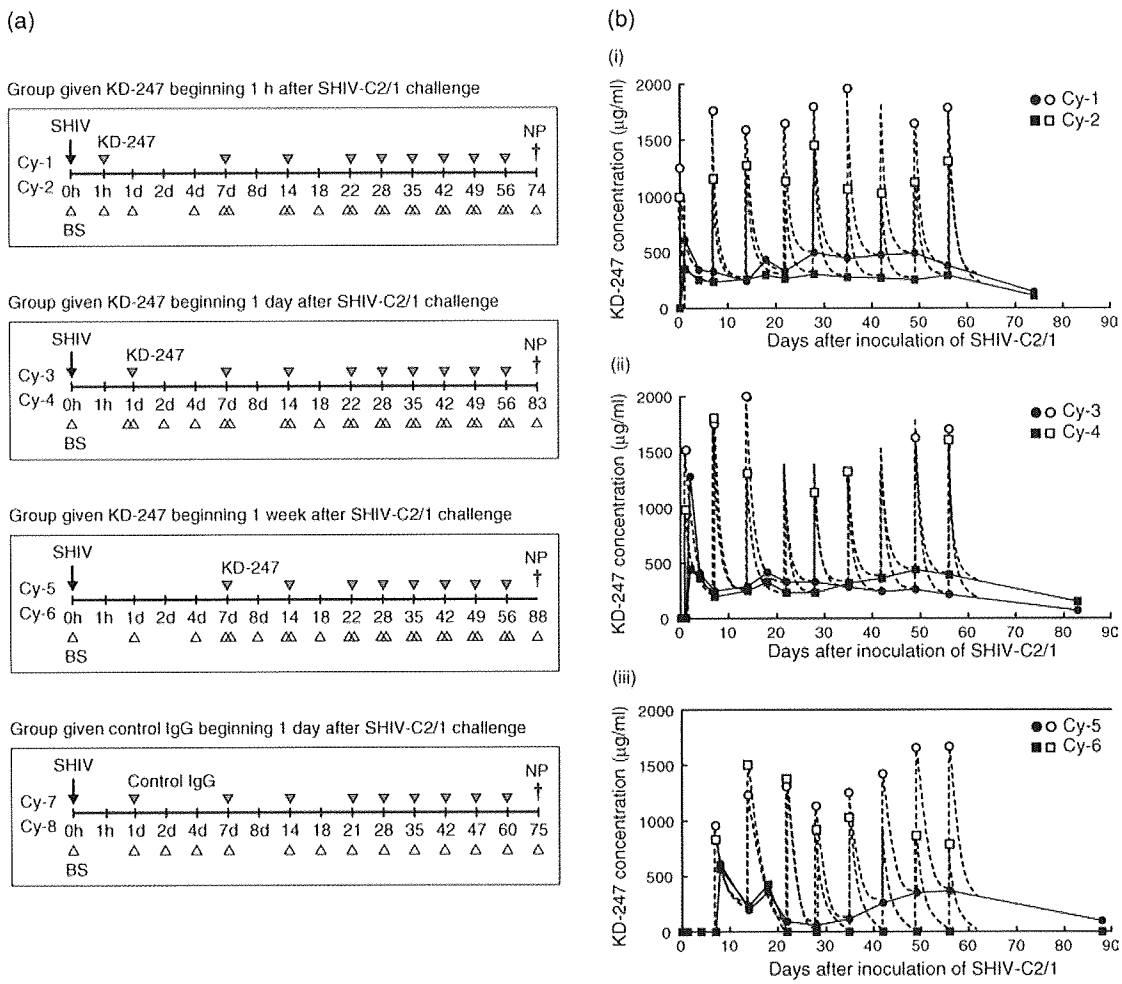

Fig. 1. KD-247 administration schedules and pharmacokinetic profiles. (a) Scheme of viral challenge and postinfection passive immunization with KD-247. A total of eight cynomolgus monkeys were used for viral infection studies with highly pathogenic SHIV-C2/1 (20 $TCID_{50}$). In the first group of two monkeys, 45 mg/kg of KD-247 was intravenously administered at 1 h after viral challenge and antibody administered once per week for 2 months. Monkeys in the second and third groups were injected with antibody at 1 day and 1 week after viral challenge, respectively, and similarly treated with the antibody. Monkeys in the fourth group were injected with 45 mg/kg of human normal immunoglobulin fraction at 1 day after viral challenge followed by passive transfer of this control IgG once a week for 2 months. Two other monkeys were used as positive controls for infection by SHIV-C2/1 with 20 $TCID_{50}$ without passive transfer of antibody, whereas 15 other monkeys were used as naive controls without viral infection and antibody transfer. (b) KD-247 concentrations in the plasma of monkeys treated 1 h (i), 1 day (ii), or 1 week (iii) after SHIV-C2/1 challenge. Closed and open symbols indicate KD-247 concentrations in plasma collected immediately before and 15 min after administration of KD-247, respectively. Broken lines show the estimated changes in KD-247 concentrations. BS, blood sampling; NP, necropsy; SHIV-C2/1, simian/human immunodeficiency virus C2/1; $TCID_{50}$, 50% tissue culture infective dose.

stopped. The plates were measured for optical density at 450 nm with a precision microplate reader (Emax; Molecular Devices, Menlo Park, California, USA). The concentrations of KD-247 antibody in the plasma were evaluated from a calibration curve drawn with software developed for the reader (SOFTmax; Molecular Devices).

Detection of anti-KD-247 antibodies

Anti-KD-247 antibodies in plasma were detected using 96-well ELISA plates (MaxiSorp) coated with KD-247. After washing and blocking, samples containing test monkey plasma at 1 : 400 dilution or a positive control were then added and incubated. A positive control was pooled with rabbit anti-KD-247 plasma at 1 : 4000 dilution. The wells were washed, incubated with biotinylated KD-247, and then washed again. Peroxidase-conjugated streptavidin (Sigma Chemical, St. Louis, Missouri, USA) was diluted and added to the wells for reaction.

Real-time reverse transcriptase-PCR quantitation of simian/human immunodeficiency virus RNA in plasma

Plasma viral loads were evaluated by real-time reverse transcriptase PCR (RT-PCR) as described previously

Copyright © Lippincott Williams & Wilkins. Unauthorized reproduction of this article is prohibited.

[17,18]. Viral RNA in plasma was extracted and purified using the QIAamp Viral RNA Mini Kit (Qiagen, Valencia, California, USA). For quantitative analysis of the RNA, the TaqMan system (Applied Biosystems, Foster City, California, USA) was used with primers and probes targeting the SIVmac239 *gag* region. The viral RNA was amplified using TaqMan EZ RT-PCR Kit (Applied Biosystems) with primers. The RT-PCR product was quantitatively monitored by its fluorescent intensity with ABI7700 (Applied Biosystems). Plasma viral load, which was measured in duplicate, was calculated based on the standard curve of control RNA and RNA recovery rate. The limit of detection was approximately 500 RNA copies/ml.

Flow cytometric evaluation of cell surface antigen expression and absolute cell count

Lymphoid cells for flow cytometric analyses were prepared from intact thymuses, spleens, and lymph nodes. Mouse mAbs conjugated with either fluorescein isothiocyanate (FITC), phycoerythrin, phycoerythrin-Cy5, or peridinin chlorophyll protein (PerCP) were used in flow cytometric analyses to detect cellular expression of monkey CD3 (NF-18; BioSource International, Camarillo, California, USA), human CD4 (SK3; Becton Dickinson, San Jose, California, USA), and CD8 (SK1; Becton Dickinson). To determine absolute cell counts, samples of whole blood were analyzed following the addition of FITC-conjugated anti-CD3 (BioSource), phycoerythrin-conjugated anti-CD4 (Becton Dickinson), and PerCP-conjugated anti-CD8 mAbs (Becton Dickinson), as previously described [19].

Results

KD-247 concentrations and detection of anti-KD-247 antibodies in monkey plasma

Blood was drawn from monkeys before and after the administration of KD-247 and at necropsy (Fig. 1a). In the monkeys that were given antibody beginning 1 h (Cy-1 and Cy-2) or 1 day (Cy-3 and Cy-4) after challenge with SHIV-C2/1, concentrations of KD-247 peaked at 800–2000 μg/ml at 15 min after injection and were maintained at 200–500 μg/ml until the next administration (as evidenced in blood samples drawn before each administration and within 15 min of the injection) (Fig. 1b i and ii). The plasma concentrations of KD-247 in monkeys treated beginning 1 week after challenge with the virus (Cy-5 and Cy-6) did not remain constant. In particular, the KD-247 maintenance concentrations in Cy-6 after day 22 were below the limit of detection (2.5 μg/ml) of the assay (Fig. 1b iii).

Because KD-247 was repeatedly administered to the monkeys, we also considered the possibility of anti-KD-247 antibody production. Anti-KD-247 antibodies in monkey plasma (1 : 400 dilution) were measured using samples collected at necropsy. Binding activity indicated that the number of anti-KD-247 antibodies in Cy-6 was significantly higher than in the other monkeys (Fig. 2a). To clarify the sites of recognition of the anti-KD-247 antibodies in Cy-6, the binding activity of antibodies in Cy-6 plasma to other anti-HIV-1 antibodies was investigated. Rμ5.5 is a reshaped mAb that is equivalent to the entire KD-247 molecule except for antigen-binding sites [6,20], and Cβ1 is a chimeric mAb whose Fc region is equivalent to that of KD-247 [21]. These mAbs were used, as well as KD-247 coated for ELISA. The reaction of these mAbs with the monkey antibodies was detected by biotinylated KD-247 based on a double-antibody capture ELISA. The antibodies bound to KD-247 in Cy-6 plasma reacted with neither Rμ5.5 nor Cβ1 (Fig. 2b). Finally, we examined whether anti-KD-247 antibodies in Cy-6 plasma inhibit the binding of KD-247 to antigen peptides. Two KD-247-specific antigen peptides, SP13 and P20PATH (NNTRRRLSIGPGRA-FYARRN), derived from the V3 region of SHIV-C2/1, were coated on ELISA plates and reacted with KD-247 that had been incubated overnight at 4°C with Cy-6 plasma collected on day 0, day 7, or at necropsy. Binding of KD-247 to antigen peptides decreased by approximately 60% after reaction of mAb with Cy-6 plasma collected at necropsy (Fig. 2c). Antibody inhibition of the binding of KD-247 to antigen peptides strongly suggests that the plasma contained an antiidiotype antibody.

Suppression of plasma viral load and of $CD4^+$ T-cell loss in peripheral blood

The kinetics of plasma viral load in monkey plasma is shown in Fig. 3(a). The viral loads were suppressed in monkeys given KD-247 in comparison with those given control IgG. The complete protection previously reported with preadministration of KD-247 was not achieved in these postadministration trials [7]. The $CD4^+$ T-cell counts were maintained at higher levels in monkeys given KD-247 than in the control animals (Fig. 3b). The suppression of viral load and the maintenance effect of KD-247 on $CD4^+$ T cells were similar among the test groups. As each group had only two animals, between-group significant differences were not tested.

Maintenance of $CD4^+$ T cells in various lymphoid tissues

At 11–13 weeks after viral challenge, necropsies of the monkeys given KD-247 were performed and their lymphoid organs were evaluated. All the lymph nodes of the monkeys inoculated with pathogenic SHIV followed by control IgG were atrophied. In contrast, the lymph nodes of all monkeys given KD-247 maintained normal shape. Marked change was observed in the thymus (Fig. 4a); the thymuses of all monkeys given KD-247 were hypertrophic, whereas the thymuses of monkeys inoculated with SHIV alone, or given control IgG, were atrophied. No organ atrophy was observed in any of the

Copyright © Lippincott Williams & Wilkins. Unauthorized reproduction of this article is prohibited.

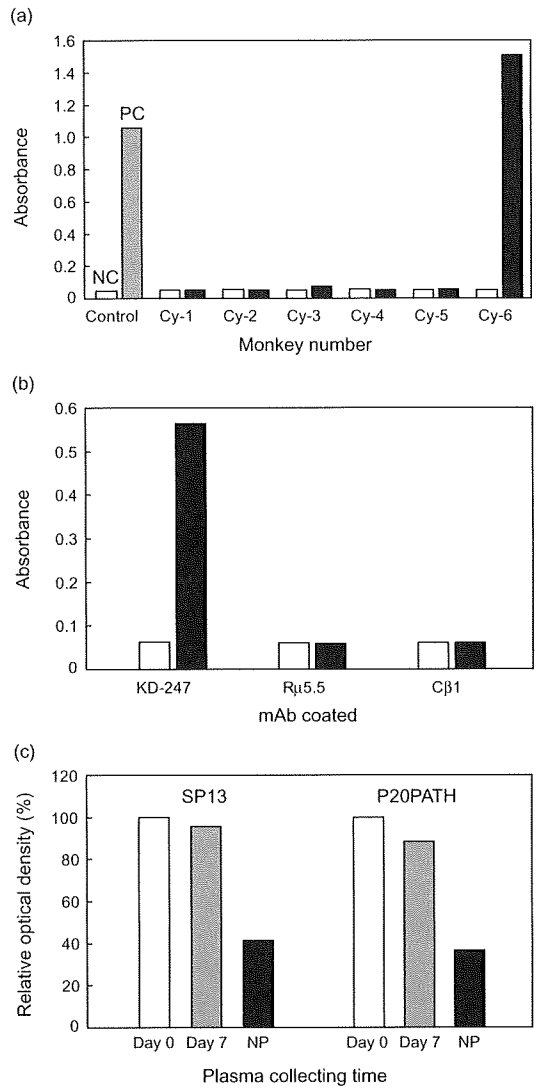

Fig. 2. Properties of anti-KD-247 antibodies in Cy-6 monkey plasma. (a) Anti-KD-247 activity of plasma in monkeys given KD-247. Open and closed bars indicate the binding activities of anti-KD-247 antibodies to KD-247 in monkey plasma collected at day 0 and necropsy, respectively. NC, negative control using the sample diluent; PC, positive control using a goat antibody to human IgG (200 ng/ml; ICN/Cappel, Aurora, Ohio, USA). (b) Binding of Cy-6 plasma to humanized and chimeric mAbs. Open and closed bars indicate binding activities of anti-KD-247 antibodies to KD-247 in monkey plasma collected on day 0 and at necropsy (day 88), respectively. (c) Inhibitory effect of Cy-6 plasma on the binding of KD-247 to antigen peptides SP13 (left) and P20PATH (right). The plasma samples collected on day 7 and at necropsy had been incubated with these peptides. Suppression of the binding of KD-247 to the peptides is shown as relative optical density (%) to the binding of KD-247 incubated with plasma collected on day 0. IgG, immunoglobulin G; NP, necropsy.

groups treated with KD-247. To determine the architecture of the lymph nodes, we examined tissue sections collected at necropsy. Germinal centers were not detected in the lymphoid tissue of monkeys treated with control IgG, but cell architecture was preserved in monkeys given KD-247 (Fig. 4b).

The T-cell subpopulation in the lymphoid tissues of the monkeys was analyzed by flow cytometry (Fig. 5). The $CD4^+$ T cells in the lymph nodes of both the IgG control monkeys (Cy-7 and Cy-8) were nearly depleted. In contrast, a normal level of $CD4^+CD8^-$ cells was maintained in the lymph nodes of all monkeys given KD-247. The $CD4^+CD8^-$ T-cell population values in the groups given KD-247 and control IgG were obviously higher and lower, respectively, than the values for the mean − 2 SD in naive control monkeys ($n = 15$). In the thymus, the absolute cell numbers of the monkeys given control IgG were low and could not be assessed for Cy-7 lymphocytes because of cell depletion. Thymic T-cell subpopulations were composed almost entirely of $CD4^+CD8^+$ double-positive cells (Cy-1 = 52%, Cy-2 = 74%, Cy-3 = 75%, Cy-4 = 76%, Cy-5 = 77%, Cy-6 = 75%, and Cy-8 = 71%; naive = 63 ± 15%). In the submandibular and mesenteric lymph nodes and spleen, administration of KD-247 rescued $CD4^+CD8^-$ cells independently of injection timing; this T-cell subset was not maintained in IgG controls.

Discussion

Since the development of HAART, the likelihood of progression to AIDS or death has been decreased if $CD4^+$ T-cell counts are properly maintained even when HIV-1 RNA concentrations in peripheral blood are high [22]. This finding suggests importance of maintaining $CD4^+$ T cells in the whole body for the control of HIV/AIDS. In this study, we confirmed that postinfection passive immunization of SHIV-infected monkeys with KD-247 fully rescued $CD4^+$ T-cell loss in various lymphoid tissues and yielded partial protection against increased plasma viral load and loss of $CD4^+$ T cells.

How, then, does postinfection immunization with KD-247 help maintain $CD4^+$ T cells in lymphoid tissues? Immunohistological alterations of the lymph nodes in HIV-infected patients represent a dynamic process, in which an initial florid follicular hyperplasia gives way ultimately to lymphocyte depletion [23]. There are several theories regarding the various direct or indirect mechanisms of $CD4^+$ lymphocyte depletion by HIV [24]. We previously reported that treatment with the humanized neutralizing antibody Rμ5.5 prevented HIV-1-induced atrophic changes in the medulla of engrafted thymic tissue in a thymus/liver-transplanted severe combined immunodeficient murine model [20]. The acute pathogenic SHIV-C2/1-derived clone virus KS661 resulted in increased thymic involution, atrophy, and the depletion of immature T cells, including $CD4^+CD8^+$ double-positive cells [25]. Infection with HIV-1, SIV, or

Copyright © Lippincott Williams & Wilkins. Unauthorized reproduction of this article is prohibited.

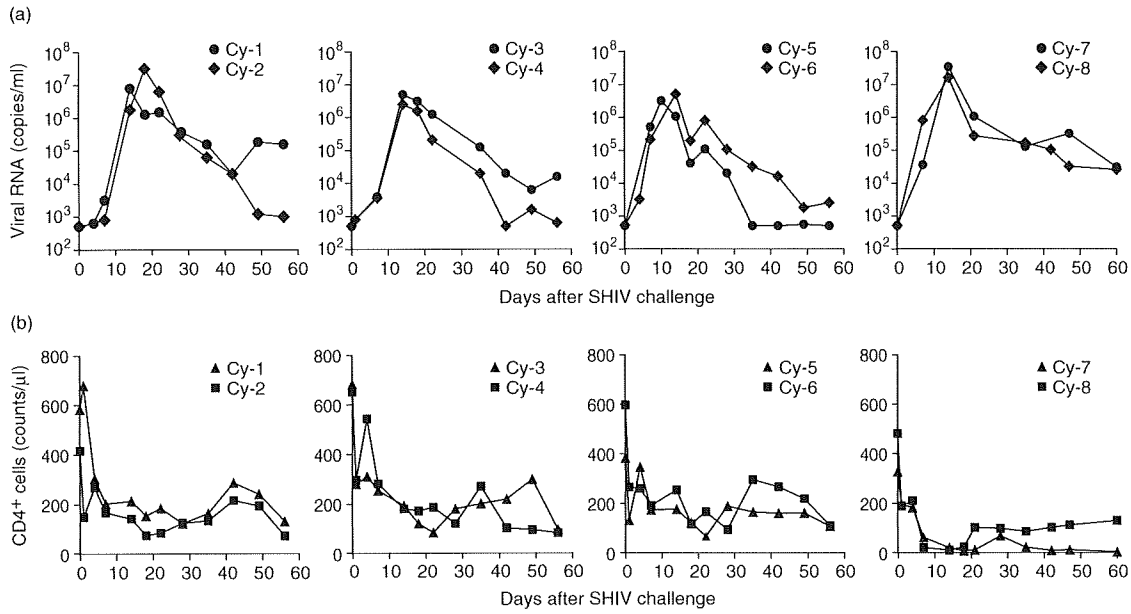

Fig. 3. Plasma viral loads and CD4$^+$ T-cell counts after viral challenge. Postchallenge plasma viral RNA copies and absolute CD4$^+$ T-cell counts in the peripheral blood were detected in the monkeys in each of four groups treated with KD-247 antibody or control IgG after infection as described in Fig. 1(a). (a) Kinetic changes in viral RNA copy numbers per ml of peripheral blood. (b) Kinetics of CD4$^+$ T-cell counts. IgG, immunoglobulin G; SHIV, simian/human immunodeficiency virus.

SHIV is associated with abnormalities in the number, size, and structure of germinal centers [26]. Progressive depletion of proliferating B cells and disruption of the follicular dendritic cell network in germinal centers within 20 days after SIV challenge have also been reported [27]. Although our study was limited by small group size (two monkeys/group), our data clearly show only minimal differences in CD4$^+$ T-cell levels between groups treated with KD-247 and the IgG control monkeys. The effects of KD-247 on CD4$^+$ T cells were more remarkable in lymph node than in peripheral blood compartments. Accumulation of apoptotic cells has been reported in both lymph nodes and thymus during the second week of highly pathogenic SHIV-C2/1 [17,28] and $SHIV_{DH12R}$ infections [29]. Given the smaller increase in CD4$^+$CD95$^+$ cell populations in peripheral blood mononuclear cells among monkeys that exhibited even partial protection from postchallenge SHIV-C2/1 with a suboptimal dose of KD-247 infusion in previous studies [7], KD-247 might protect against apoptosis of CD4$^+$ T cells in lymphoid tissues. Thus, in addition to neutralizing antibodies in animals receiving transfusions, passive transfer of KD-247 might help to maintain levels of CD4$^+$ T cells and to preserve the integrity of lymphoid structures, potentially leading to a less pathogenic course of disease progression. The roles played by the antibodies against HIV/AIDS could be clarified by further analyses of immunological function of monkeys treated with KD-247; areas of future research include viral components [30,31], lymphocyte activation [32,33], cytokine spectra [34], T-cell homeostasis [35,36], dendritic cell functions [37,38], Fc receptor interactions [39,40], and related functions.

Because preinfection experiments have shown that the concentration of KD-247 in plasma is important in protecting monkeys against viral infection [7], we also measured KD-247 concentrations in plasma samples. The postinfection effect of KD-247 against increased viral load and CD4$^+$ T-cell loss in peripheral blood were evaluated. Monkeys given KD-247 had lower plasma viral loads and less CD4$^+$ T-cell loss than did those treated with control IgG; however, as noted above, each group had only two animals and no statistical analysis was performed. These results in peripheral blood were not very pronounced compared with the phenomena observed in lymphoid organs. Complete protection, which was previously reported with preinfection administration of KD-247 [7], was not achieved in these postinfection trials. The times and values of viral load peaks were similar in all monkeys, but the increases in viral loads were delayed by administration of KD-247. Interestingly, the ability of KD-247 to suppress viral loads after they peaked did not depend on the timing of administration. In previous preinfection experiments with 45 mg/kg of KD-247, viral challenges were performed 1 day after KD-247 administration, and blood concentrations of KD-247 ranged from 700 to 800 μg/ml immediately before viral challenge in monkeys. Preadministration of these concentrations of KD-247 yielded complete protection against SHIV-C2/1 infection [7]. By contrast, in the current study, the monkeys given KD-247 1 h after

Copyright © Lippincott Williams & Wilkins. Unauthorized reproduction of this article is prohibited.

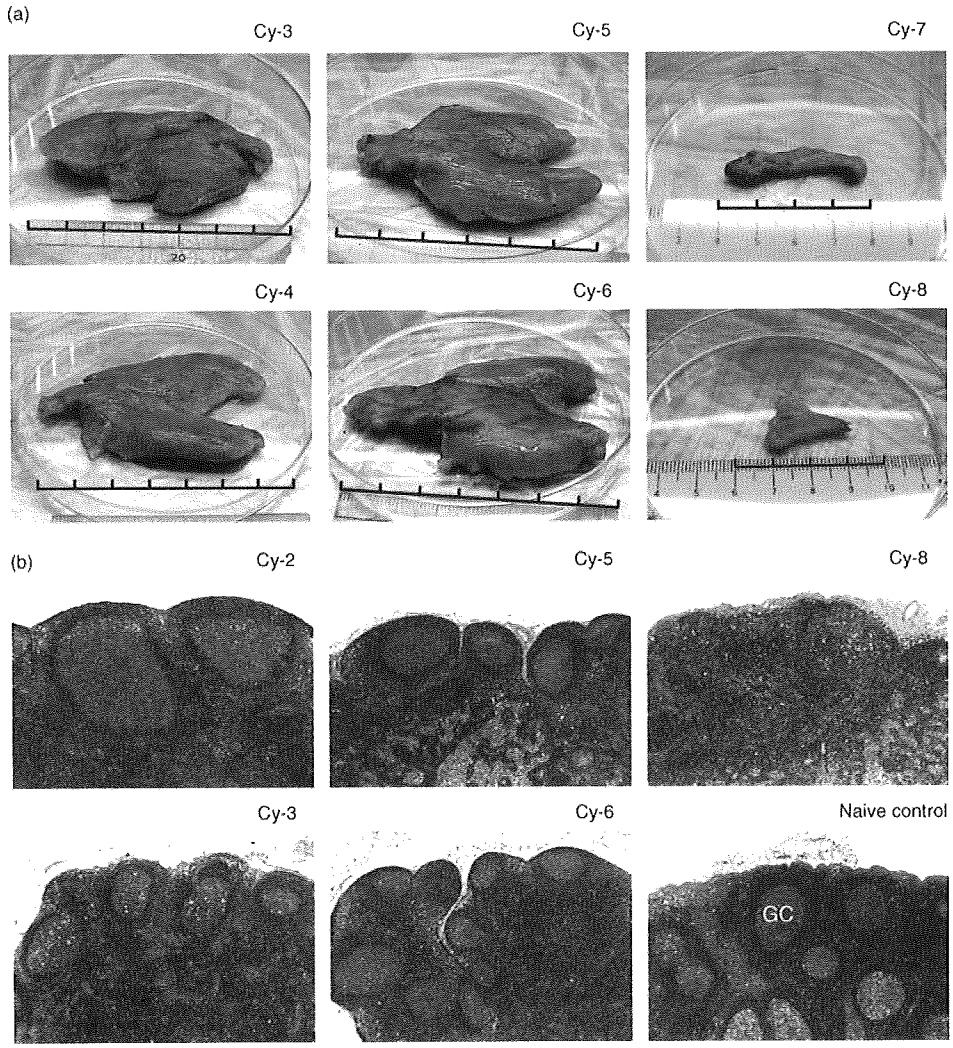

Fig. 4. Comparative postinfection protection against atrophic changes in lymphoid tissues. (a) Macroscopic images of thymus. Superimposed rulers indicate scales marked in centimeters. Although Cy-1, Cy-2, and naive control thymuses are not shown here, all thymuses of the monkeys given KD-247 were larger and those given control IgG were smaller than naive monkey thymuses. (b) Histological changes as postinfection effects of KD-247. Parts of the tissue blocks were preserved in 10% buffered formalin, embedded in paraffin. Tissue sections were stained with hematoxylin and eosin for conventional light microscopy (original magnification 18×). Mesenteric (Cy-2, Cy-5, and Cy-6), inguinal (Cy-3 and naive control), and submandibular (Cy-8) lymph nodes were photographed. Germinal centers, which are bright round areas (shown as GC in only the naive control), were maintained in the monkeys given KD-247, whereas the architecture of germinal centers in lymph node tissue from the control monkey given human normal IgG was not detected. GC, germinal centers; IgG, immunoglobulin G.

challenge with the virus became infected, even though the KD-247 concentrations 15 min after administration ranged from 1000 to 1300 μg/ml (Fig. 1b i). These KD-247 concentrations are considered sufficient to neutralize cell-free viruses that develop after the initial infection and/or are generated one after another following infection in peripheral blood. Therefore, the inability of the antibody administered 1 h after challenge to completely protect against the virus suggests that target cells were infected with the virus within 1 h. The previously reported results of time-dependence studies [10,11,41] of postinfection prophylaxis using SHIV are comparable with those obtained in the present study. The virus might not only infect target cells directly but also evade neutralizing antibody to produce infection in the cells of the peripheral blood and/or the lymphoid tissues [42,43]. Follicular dendritic cells could sustain HIV infection in the presence of neutralizing antibody [44]. Mucosal infection, such as vaginal challenge with SHIV, has been suggested to be a better in-vivo model to evaluate passive immunization [45,46]. The effects of antibodies in the lymph node compartment might be clearly observable using models of mucosal infection, as viruses harbored in lymph nodes after mucosal challenge later appeared in the peripheral blood compartment following systemic spread. Unexpectedly,

Copyright © Lippincott Williams & Wilkins. Unauthorized reproduction of this article is prohibited.

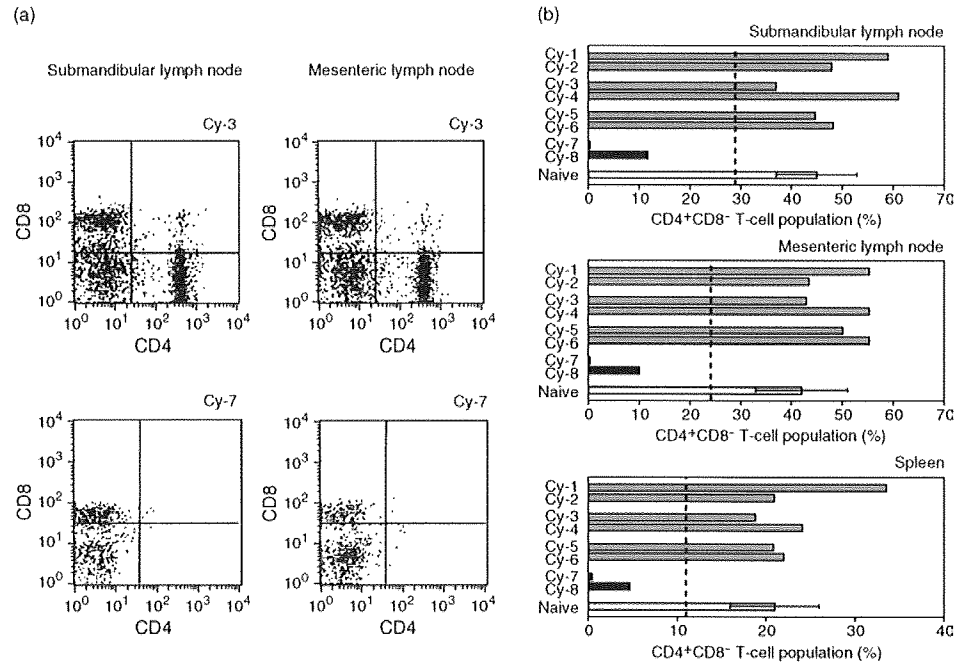

Fig. 5. Postinfection protection against tissue CD4$^+$ T-cell loss by passive transfer of KD-247 at various times after simian/human immunodeficiency virus C2/1 challenge. (a) Flow cytometric profiles of CD4$^+$ and CD8$^+$ T cells in the submandibular (left) and mesenteric (right) lymph nodes. Upper panels show maintenance of CD4$^+$ T cells in animal Cy-3 after passive transfer of KD-247. Lower panels show the loss of CD4$^+$ populations in the control IgG-treated animal Cy-7. (b) Postinfection protection of KD-247 against loss of CD4$^+$CD8$^-$ tissue lymphocytes. Tissue distributions of CD4$^+$CD8$^-$ T cells were determined in submandibular and mesenteric lymph nodes and spleen in animals of each group, as well as in those of naive control monkeys ($n = 15$). Bars indicate SD. Broken lines show the mean – 2 SD values of the naive control. IgG, immunoglobulin G.

the maintenance of CD4$^+$ T cells in the lymph nodes in Cy-6 were similar to those in the other monkeys given KD-247, although the mAb was eliminated from the plasma 3 weeks after viral challenge, once anti-KD-247 antibodies were elicited in this monkey. High plasma concentrations of KD-247 seem to be effective in preventing HIV-1 transmission. However, even if high concentrations are not maintained in the blood for a long time, KD-247 could rescue lymphoid CD4$^+$ T cells.

Passive immunization with mAbs has been shown to prevent a variety of diseases, although no mAb products are licensed for use for immunotherapy against HIV/AIDS [47]. In a passive immunization trial with humans, a cocktail of three mAbs was able to delay viral rebound following interruption of antiretroviral therapy [15]. However, differences in the pharmacokinetic profiles of constituent mAbs and cost-related issues of production might affect the development of neutralizing mAb cocktail drugs [47,48]. In contrast, KD-247 itself neutralizes primary isolates including chemokine (C–C motif) receptor 5 (CCR5)-tropic viruses with a matching narrow-neutralization sequence motif [6,7]. KD-247 is expected to be useful as a novel reagent for immune protection against HIV/AIDS, because the mAb might not only directly neutralize the virus but also maintain CD4$^+$ T cells in lymphoid tissues.

Acknowledgements

This work was supported by the 'Panel on AIDS' of the United States–Japan Cooperative Medical Science Program and the Health Science Foundation, Japan.

T. Murakami planned experiments, wrote the manuscript, and analyzed the laboratory data; M. Honda conducted the study, planned the experiments, and wrote the manuscript; Y. Eda planned and conducted the experiments; T. Nakasone, K. Someya, N. Yoshino, M. Kaizu, and Y. Izumi performed the animal experiments and analyzed the laboratory data; Y. Ami and H. Matsui performed the animal experiments and the pathological analyses; K. Shinohara managed the animal experiments; N. Yamamoto supervised the study.

Part of the information was presented at the 16th Annual Meeting of the Japanese Society for AIDS Research, 28–30 November 2002, Nagoya, Japan (abstract 249).

References

1. Douek DC, Kwong PD, Nabel GJ. **The rational design of an AIDS vaccine.** *Cell* 2006; **124**:677–681.
2. McMichael AJ. **HIV vaccines.** *Annu Rev Immunol* 2006; **24**: 227–255.

Copyright © Lippincott Williams & Wilkins. Unauthorized reproduction of this article is prohibited.

3. Haynes BF, Montefiori DC. **Aiming to induce broadly reactive neutralizing antibody responses with HIV-1 vaccine candidates.** *Expert Rev Vaccines* 2006; **5**:579–595.
4. Lin G, Nara PL. **Designing immunogens to elicit broadly neutralizing antibodies to the HIV-1 envelope glycoprotein.** *Curr HIV Res* 2007; **5**:514–541.
5. Emini EA, Schleif WA, Nunberg JH, Conley AJ, Eda Y, Tokiyoshi S, *et al.* **Prevention of HIV-1 infection in chimpanzees by gp120 V3 domain-specific monoclonal antibody.** *Nature* 1992; **355**:728–730.
6. Eda Y, Takizawa M, Murakami T, Maeda H, Kimachi K, Yonemura H, *et al.* **Sequential immunization with V3 peptides from primary human immunodeficiency virus type 1 produces cross-neutralizing antibodies against primary isolates with a matching narrow-neutralization sequence motif.** *J Virol* 2006; **80**: 5552–5562.
7. Eda Y, Murakami T, Ami Y, Nakasone T, Takizawa M, Someya K, *et al.* **Anti-V3 humanized antibody KD-247 effectively suppresses ex vivo generation of human immunodeficiency virus type 1 and affords sterile protection of monkeys against a heterologous simian/human immunodeficiency virus infection.** *J Virol* 2006; **80**:5563–5570.
8. Matsushita S, Takahama S, Shibata J, Kimura T, Shiosaki K, Eda Y, *et al.* **Ex vivo neutralization of HIV-1 quasi-species by a broadly reactive humanized monoclonal antibody KD-247.** *Hum Antibodies* 2005; **14**:81–88.
9. Haigwood NL, Montefiori DC, Sutton WF, McClure J, Watson AJ, Voss G, *et al.* **Passive immunotherapy in simian immunodeficiency virus-infected macaques accelerates the development of neutralizing antibodies.** *J Virol* 2004; **78**:5983–5995.
10. Nishimura Y, Igarashi T, Haigwood NL, Sadjadpour R, Donau OK, Buckler C, *et al.* **Transfer of neutralizing IgG to macaques 6 h but not 24 h after SHIV infection confers sterilizing protection: implications for HIV-1 vaccine development.** *Proc Natl Acad Sci U S A* 2003; **100**:15131–15136.
11. Ferrantelli F, Buckley KA, Rasmussen RA, Chalmers A, Wang T, Li P-L, *et al.* **Time dependence of protective postexposure prophylaxis with human monoclonal antibodies against pathogenic SHIV challenge in newborn macaques.** *Virology* 2007; **358**:69–78.
12. Ruprecht RM, Ferrantelli F, Kitabwalla M, Xu W, McClure HM. **Antibody protection: passive immunization of neonates against oral AIDS virus challenge.** *Vaccine* 2003; **21**:3370–3373.
13. Safrit JT, Ruprecht R, Ferrantelli F, Xu W, Kitabwalla M, Van Rompay K, *et al.*, Ghent IAS Working Group on HIV in Women and Children. **Immunoprophylaxis to prevent mother-to-child transmission of HIV-1.** *J Acquir Immune Defic Syndr* 2004; **35**:169–177.
14. Hammer SM, Saag MS, Schechter M, Montaner JSG, Schooley RT, Jacobsen DM, *et al.*, International AIDS Society-USA panel. **Treatment for adult HIV infection: 2006 recommendations of the International AIDS Society-USA panel.** *JAMA* 2006; **296**: 827–843.
15. Trkola A, Kuster H, Rusert P, Joos B, Fischer M, Leemann C, *et al.* **Delay of HIV-1 rebound after cessation of antiretroviral therapy through passive transfer of human neutralizing antibodies.** *Nat Med* 2005; **11**:615–622.
16. Shinohara K, Sakai K, Ando S, Ami Y, Yoshino N, Takahashi E, *et al.* **A highly pathogenic simian/human immunodeficiency virus with genetic changes in cynomolgus monkey.** *J Gen Virol* 1999; **80**:1231–1240.
17. Sasaki Y, Ami Y, Nakasone T, Shinohara K, Takahashi E, Ando S, *et al.* **Induction of CD95 ligand expression on T lymphocytes and B lymphocytes and its contribution to apoptosis of CD95-up-regulated CD4$^+$ T lymphocytes in macaques by infection with a pathogenic simian/human immunodeficiency virus.** *Clin Exp Immunol* 2000; **122**:381–389.
18. Kaizu M, Sato H, Ami Y, Izumi Y, Nakasone T, Tomita Y, *et al.* **Infection of macaques with an R5-tropic SHIV bearing a chimeric envelope carrying subtype E V3 loop among subtype B framework.** *Arch Virol* 2003; **148**:973–988.
19. Yoshino N, Ami Y, Terao K, Tashiro F, Honda M. **Upgrading of flow cytometric analysis for absolute counts, cytokines and other antigenic molecules of cynomolgus monkeys (*Macaca fascicularis*) by using antihuman cross-reactive antibodies.** *Exp Anim* 2000; **49**:97–110.
20. Okamoto Y, Eda Y, Ogura A, Shibata S, Amagai T, Katsura Y, *et al.* **In SCID-hu mice, passive transfer of a humanized antibody prevents infection and atrophic change of medulla in human thymic implant due to intravenous inoculation of primary HIV-1 isolate.** *J Immunol* 1998; **160**:69–76.
21. Matsushita S, Maeda H, Kimachi K, Eda Y, Maeda Y, Murakami T, *et al.* **Characterization of a mouse/human chimeric monoclonal antibody (Cβ1) to a principal neutralizing domain of the human immunodeficiency virus type 1 envelope protein.** *AIDS Res Hum Retroviruses* 1992; **8**:1107–1115.
22. Egger M, May M, Chêne G, Phillips AN, Ledergerber B, Dabis F, *et al.*, and the ART Cohort Collaboration. **Prognosis of HIV-1-infected patients starting highly active antiretroviral therapy: a collaborative analysis of prospective studies.** *Lancet* 2002; **360**:119–129.
23. Wood GS. **The immunohistology of lymph nodes in HIV infection: a review.** *Prog AIDS Pathol* 1990; **2**:25–32.
24. Cloyd MW, Chen JJY, Adeqboyega P, Wang L. **How does HIV cause depletion of CD4 lymphocytes? A mechanism involving virus signaling through its cellular receptors.** *Curr Mol Med* 2001; **1**:545–550.
25. Motohara M, Ibuki K, Miyake A, Fukazawa Y, Inaba K, Suzuki H, *et al.* **Impaired T-cell differentiation in the thymus at the early stages of acute pathogenic chimeric simian-human immunodeficiency virus (SHIV) infection in contrast to less pathogenic SHIV infection.** *Microbes Infect* 2006; **8**:1539–1549.
26. Margolin DH, Saunders EH, Bronfin B, de Rosa N, Axthelm MK, Goloubeva OG, *et al.* **Germinal center function in the spleen during simian HIV infection in rhesus monkeys.** *J Immunol* 2006; **177**:1108–1119.
27. Zhang Z-Q, Casimiro DR, Schleif WA, Chen M, Citron M, Davies M-E, *et al.* **Early depletion of proliferating B cells of germinal center in rapidly progressive simian immunodeficiency virus infection.** *Virology* 2007; **361**:455–464.
28. Yoshino N, Ryu T, Sugamata M, Ihara T, Ami Y, Shinohara K, *et al.* **Direct detection of apoptotic cells in peripheral blood from highly pathogenic SHIV-inoculated monkey.** *Biochem Biophys Res Commun* 2000; **268**:868–874.
29. Igarashi T, Brown CR, Byrum RA, Nishimura Y, Endo Y, Plishka RJ, *et al.* **Rapid and irreversible CD4$^+$ T-cell depletion induced by the highly pathogenic simian/human immunodeficiency virus SHIV$_{DH12R}$ is systemic and synchronous.** *J Virol* 2002; **76**:379–391.
30. Gratton S, Cheynier R, Dumaurier M-J, Oksenhendler E, Wain-Hobson S. **Highly restricted spread of HIV-1 and multiply infected cells within splenic germinal centers.** *Proc Natl Acad Sci U S A* 2000; **97**:14566–14571.
31. de Paiva GR, Laurent C, Godel A, da Silva NA Jr, March M, Delsol G, *et al.* **Discovery of human immunodeficiency virus infection by immunohistochemistry on lymph node biopsies from patients with unexplained follicular hyperplasia.** *Am J Surg Pathol* 2007; **31**:1534–1538.
32. Zamarchi R, Barelli A, Borri A, Petralia G, Ometto L, Masiero S, *et al.* **B cell activation in peripheral blood and lymph nodes during HIV infection.** *AIDS* 2002; **16**:1217–1226.
33. Biancotto A, Iglehart SJ, Vanpouille C, Condack CE, Lisco A, Ruecker E, *et al.* **HIV-1-induced activation of CD4$^+$ T cells creates new targets for HIV-1 infection in human lymphoid tissue ex vivo.** *Blood* 2008; **111**:699–704.
34. Biancotto A, Grivel J-C, Iglehart SJ, Vanpouille C, Lisco A, Sieg SF, *et al.* **Abnormal activation and cytokine spectra in lymph nodes of people chronically infected with HIV-1.** *Blood* 2007; **109**:4272–4279.
35. Nokta MA, Li X-D, Nichols J, Pou A, Asmuth D, Pollard RB. **Homeostasis of naive and memory T cell subpopulations in peripheral blood and lymphoid tissues in the context of human immunodeficiency virus infection.** *J Infect Dis* 2001; **183**:1336–1342.
36. Letvin NL, Mascola JR, Sun Y, Gorgone DA, Buzby AP, Xu L, *et al.* **Preserved CD4$^+$ central memory T cells and survival in vaccinated SIV-challenged monkeys.** *Science* 2006; **312**:1530–1533.
37. Taruishi M, Terashima K, Dewan Z, Dewan MZ, Yamamoto N, Ikeda S, *et al.* **Role of follicular dendritic cells in the early HIV-1 infection: in vitro model without specific antibody.** *Microbiol Immunol* 2004; **48**:693–702.

Copyright © Lippincott Williams & Wilkins. Unauthorized reproduction of this article is prohibited.

38. Turville SG, Aravantinou M, Stössel H, Romani N, Robbiani M. **Resolution of de novo HIV production and trafficking in immature dendritic cells.** *Nat Methods* 2008; **5**:75–85.
39. Forthal DN, Landucci G, Phan TB, Becerra J. **Interactions between natural killer cells and antibody Fc result in enhanced antibody neutralization of human immunodeficiency virus type 1.** *J Virol* 2005; **79**:2042–2049.
40. Wilflingseder D, Banki Z, Garcia E, Pruenster M, Pfister G, Muellauer B, *et al.* **IgG opsonization of HIV impedes provirus formation in and infection of dendritic cells and subsequent long-term transfer to T cells.** *J Immunol* 2007; **178**:7840–7848.
41. Foresman L, Jia F, Li Z, Wang C, Stephans EB, Sahni M, *et al.* **Neutralizing antibodies administered before, but not after, virulent SHIV prevent infection in macaques.** *AIDS Res Hum Retroviruses* 1998; **14**:1035–1043.
42. Chen JJ-Y, Huang JC, Shirtliff M, Briscoe E, Ali S, Cesani F, *et al.* **CD4 lymphocytes in the blood of HIV$^+$ individuals migrate rapidly to lymph nodes and bone marrow: support for homing theory of CD4 cell depletion.** *J Leukoc Biol* 2002; **72**:271–278.
43. Malaspina A, Moir S, Nickle DC, Donoghue ET, Ogwaro KM, Ehler LA, *et al.* **Human immunodeficiency virus type 1 bound to B cells: relationship to virus replicating in CD4$^+$ T cells and circulating in plasma.** *J Virol* 2002; **76**:8855–8863.
44. Heath SL, Tew JG, Tew JG, Szakal AK, Burton GF. **Follicular dendritic cells and human immunodeficiency virus infectivity.** *Nature* 1995; **377**:740–744.
45. Kahn JO, Walker BD. **Acute human immunodeficiency virus type 1 infection.** *N Engl J Med* 1998; **339**:33–39.
46. Mascola JR. **Passive transfer studies to elucidate the role of antibody-mediated protection against HIV-1.** *Vaccine* 2002; **20**:1922–1925.
47. Bansal GP. **A summary of the workshop on passive immunization using monoclonal antibodies for HIV/AIDS, held at the National Institute of Allergy and Infectious Diseases, Bethesda, 10 March 2006.** *Biologicals* 2007; **35**:367–371.
48. Joos B, Trkola A, Kuster H, Aceto L, Fischer M, Stiegler G, *et al.* **Long-term multiple-dose pharmacokinetics of human monoclonal antibodies (mAbs) against human immunodeficiency virus type 1 envelope gp120 (mAb 2G12) and gp41 (mAbs 4E10 and 2F5).** *Antimicrob Agents Chemother* 2006; **50**:1773–1779.

Copyright © Lippincott Williams & Wilkins. Unauthorized reproduction of this article is prohibited.

Vaccine 27 (2009) 4808–4817

Contents lists available at ScienceDirect

Vaccine

journal homepage: www.elsevier.com/locate/vaccine

Co-administration of cholera toxin and apple polyphenol extract as a novel and safe mucosal adjuvant strategy

Naoto Yoshino[a,*], Kohtaro Fujihashi[b], Yukari Hagiwara[c], Hiroyuki Kanno[d], Kiyomi Takahashi[a], Ryoki Kobayashi[b], Noriyuki Inaba[e], Masatoshi Noda[f], Shigehiro Sato[a]

[a] Department of Microbiology, School of Medicine, Iwate Medical University, 19-1 Uchimaru, Morioka, Iwate 020-8505, Japan
[b] Departments of Pediatric Dentistry and Microbiology, Immunobiology Vaccine Center, Institute for Oral Health Research, The University of Alabama at Birmingham, Birmingham, AL 35294-0007, USA
[c] Research Center for Biologicals, The Kitasato Institute, Saitama 364-0026, Japan
[d] Department of Pathology, School of Medicine, Iwate Medical University, Iwate 020-8505, Japan
[e] Department of Obstetrics & Gynecology, School of Medicine, Dokkyo Medical University, Tochigi 321-0293, Japan
[f] Department of Molecular Infectiology, Graduate School of Medicine, Chiba University, Chiba 260-8670, Japan

ARTICLE INFO

Article history:
Received 25 February 2009
Accepted 28 May 2009
Available online 17 June 2009

Keywords:
Cholera toxin
Apple polyphenol extract
Mucosal adjuvant

ABSTRACT

Although native cholera toxin (CT) is an extremely effective adjuvant, its toxicity prevents its use in humans. We report here that apple polyphenol extract (APE), obtained from unripe apples, reduces CT-induced morphological changes and cAMP accumulation. Based upon this finding, we have attempted to design a novel, effective and safe mucosal vaccine by using CT with several dosages of APE as nasal adjuvants. Mice nasally immunized with OVA plus CT and an optimal dosage of APE showed significantly reduced levels of inflammatory responses as well as total and OVA-specific IgE antibodies when compared with mice given without APE. However, levels of both mucosal and systemic OVA-specific antibody responses were maintained. Further, APE significantly down-regulated accumulation of CT in the olfactory nerves and epithelium. In summary, an optimal dosage of APE would take full advantage of mucosal adjuvanticity of native CT without any toxicity for application in humans.

© 2009 Elsevier Ltd. All rights reserved.

1. Introduction

The enterotoxins, native cholera toxin (CT) produced by *Vibrio cholerae*, and heat-labile toxin (LT) produced by *Escherichia coli*, serve as powerful adjuvants when co-administered with unrelated proteins via mucosal routes [1–3]. These enterotoxins enhance mucosal secretory IgA (S-IgA) and systemic IgG and IgA antibody (Ab) responses to co-administered protein antigens (Ags); however, they are unsuitable for use in humans due to their toxicity. Both CT and LT cause severe diarrhea when orally administered and central nervous system (CNS) toxicity when nasally administered [4–9]. Furthermore, safety concerns were aroused when a commercial nasal vaccine using LT as an adjuvant was withdrawn from the market due to possible association with side effects such as rhinorrhea, headache and, most seriously, facial palsy [9–12].

Four principal approaches have been developed for eliminating the toxic effects of CT while retaining its efficacy as an adjuvant; some mutants and chimeric molecules were developed to avoid the risks of CT in mucosal tissues and CNS. First, recombinant CT-B was employed as a mucosal adjuvant since the A subunit of CT (CT-A) is responsible for toxicity [13,14]. Second, in order to establish molecules that are nontoxic but retain adjuvanticity, researchers have created nontoxic mutant CTs (mCTs) by substituting a single amino acid in the ADP-ribosyltransferase active center [3,15] and double mutant CTs (dmCTs) by mutating the ADP-ribosyltransferase active center and the COOH-terminal of CT-A2 to influence the movement of CT from the Golgi apparatus to the endoplasmic reticulum [16]. Though nasal immunization with CT-induced nerve growth factor-β (NGF-β), mCT E112K did not elicit any neuronal damage based upon NGF-β production in the CNS [17]. Further, native CT accumulated in the olfactory bulbs (OBs) whereas dmCT did not [16]. Third, CT-A1 was fused to a dimer of the Ig-binding D region of *Staphylococcal aureus* protein A (CTA1-DD) to avoid the binding of CT to all nuclear cells [18–20]. In this approach, CTA1-DD does not induce inflammatory responses and does not accumulate in the OBs [20]. Finally, CT-LT chimeric molecules were constructed that differed from CT in their biological and adjuvant activity [21,22]. Nasal administration of mCT-A/LT-B, one of the CT-LT chimeric molecules, did not enhance IgE Ab responses [23].

We assessed both the efficacy and safety of administering apple polyphenol extract (APE), a crude polyphenol extracted from unripe apples, together with native CT to mitigate its toxic effects. The

* Corresponding author. Tel.: +81 19 651 5111; fax: +81 19 605 8530.
E-mail address: nyoshino@iwate-med.ac.jp (N. Yoshino).

0264-410X/$ – see front matter © 2009 Elsevier Ltd. All rights reserved.
doi:10.1016/j.vaccine.2009.05.081

ability of the enzymatic and biological properties of APE has already been established [24,25]. APE inhibits ADP-ribosylation *in vitro* and reduces CT-induced fluid accumulation in the intestines of mice. Moreover, it has been reported that oligomeric and polymeric catechins in APE are the major compounds inhibiting ADP-ribosylation [24]. As to the safety of APE, an acute toxicity test and a subchronic toxicity test in rats receiving oral APE at a dosage of 2000 mg/kg showed no significant hematological, clinical, chemical, histopathological, or urinary effects [26]. Further, in a pilot study, 10 mg/kg/day of APE proved to be nontoxic to humans when administered APE orally for 8 weeks [27].

Using recombinant CTs as mucosal adjuvants has been explored by many investigators, and these strategies have been shown to be effective mucosal adjuvants with little or no toxicity. Here, we introduce a new strategy for rendering CT a clinically suitable mucosal adjuvant. Our strategy differs radically from those outlined previously because it employs native CT, not mutant or chimeric CT. In this study, we are attempting to harness the full adjuvanticity of native CT while also guarding against toxic side effects through the use of APE.

2. Materials and methods

2.1. Toxicity and bioassay of CT in vitro

APE was kindly provided by Dr. Akio Yanagida (Institute for Production Research and Development, The Nikka Whisky Distilling Co., Ltd., Chiba, Japan). Apples and preparation methods of APE were described elsewhere [28]. The ability of CT (List Biological Laboratories, Campbell, CA) with or without several concentrations of APE to induce toxic effects on cultured mouse Y-1 adrenal tumor cells was assessed as described previously [29]. The cells were examined by light microscopy for typical rounding, and the concentration of CT required to initiate cell rounding (ECi) was determined. cAMP was quantitated as described elsewhere [15]. Intracellular cAMP measurement was done with an enzyme immunoassay kit (Amersham Pharmacia Biotech, Buckinghamshire, UK). The quantity of protein was analyzed for the same samples using a Coomassie Protein Assay Reagent (PIERCE, Rockford, IL), and the levels of cAMP were expressed as pmol of cAMP/mg of protein.

2.2. Immunization of mice

Five-week-old C57BL/6 mice ($H\text{-}2^b$) were purchased from CLEA Japan, Inc. (Tokyo, Japan). Mice were acclimated to the experimental animal facility for 1 week before being used in experiments and were maintained in the facility under specific pathogen-free conditions. All experimental procedures were carried out following the guidelines established by The Committee of Animal Experiments, Iwate Medical University. For nasal immunization, the mice were lightly anesthetized with ketamine before being immunized with a 5-μl aliquot (2.5 μl/nostril) of PBS containing 100 μg of ovalbumin (OVA; Sigma–Aldrich, St. Louis, Mo) and 0.5 μg of CT with or without specified dosages of APE, with a 5-min rest between each inoculation. Mice were immunized three times at weekly intervals in all experiments. The dosage of CT and the immunization schedule were largely the same as those used in previous studies of CT as mucosal adjuvant for mice immunized nasally [3,16,22,23,30,31].

2.3. Histopathologic analysis

We assessed the inflammatory responses in the nasal cavity of mice given nasal OVA plus CT with or without specified dosages of APE. One week after the last immunization, the head of each mouse was fixed in 10% neutral-buffered formalin and subsequently immersed in 100% ethanol. After decalcification with 10% formic acid–10% formalin at room temperature for 3 days, the tissues at the frontal section were cut into 3-mm-thick slices and embedded in paraffin. Three-μm-thick histological sections were stained with hematoxylin and eosin. Histopathologic evaluation of inflammatory responses in the nasal cavity was performed using light microscopy.

The severity of the lesions in each mouse was scored on a 1-4 grade based on the thickness of the inflammatory cell layer (excluding the lymph follicle) as follows: (1) less than five cells thick; (2) 5–10 cells thick; (3) inflammatory cell layer more than 10 cells thick covering less than 30% of the mucosal surface; and (4) inflammatory cell layer more than 10 cells thick covering more than 30% of the mucosal surface of the nasal cavity. Since the first two slices from the nasal apex exhibited higher inflammatory responses in every mouse, the inflammatory grading was examined in these two sections and a mean calculated for each mouse.

2.4. ELISA for inflammatory cytokines

Mice were nasally immunized once with a 5-μl aliquot (2.5 μl/nostril) of PBS containing 100 μg of OVA and 0.5 μg of CT with or without specified dosages of APE or PBS alone as a negative control. Six hours after the immunization, nasal washes were obtained by injecting 1 ml of PBS on three occasions into the posterior opening of nasopharynx with a hypodermic needle [32]. The inflammatory cytokines (IL-1β, IL-6, and TNF-α) in the nasal wash samples were assessed by cytokine-specific ELISAs (Quantikine®; R&D Systems, Minneapolis, NE). The detection limits of the ELISA for IL-1β, IL-6, and TNF-α were 7.8, 7.8, and 23.4 pg/ml, respectively.

2.5. Real-time quantitative PCR

The levels of inflammatory cytokine mRNA expression in the nasal tissues and the CNS of mice were determined by a real-time quantitative reverse transcription PCR. Brains, nasal septums including nasal mucosa and palates including nasopharygeal-associated lymphoreticular tissue (NALT) were rapidly removed. Brains and OBs were isolated as previously described [33]. After isolation of the OBs, the brains were cut into 1-mm-thick slices, and the first two slices (containing tissue from the frontal region and basal ganglia, respectively) were used. Samples were immediately frozen in dry ice and stored at −80 °C until use. Total RNA of the samples was extracted and 1 μg of total RNA was reverse transcribed [34]. The PCR protocols and the sequences of the primers of IL-1β, IL-6, TNF-α and GADPH have been described elsewhere [34]. To confirm amplification specificity, the PCR products from each primer pair were subsequently subjected to a dissociation curve analysis. To determine normalized cytokine mRNA values, the values for IL-1β, IL-6, and TNF-α were divided by the endogenous reference GADPH values of each sample. To determine the relative quantity of cytokine mRNA levels, the normalized cytokine mRNA values were divided by the normalized calibrator values. The calibrators were obtained from the unstimulated control group (PBS alone); the cytokine mRNA level in an unstimulated control was defined as 1 arbitrary unit.

2.6. Trafficking analysis of CT

The distribution of CT in the NALT, olfactory nerves and epithelium (ON/E) and OBs were examined using acridinium-labeled CT [16,35]. Mice were nasally administered 0.5 μg of acridinium-labeled CT together with or without specified dosages of APE. After 6 h, the NALT, ON/E and OBs were isolated, and the levels of acridinium present were determined [16]. The adjuvanticity of CT was not affected by acridinium labeling. Thus, when mice were nasally

immunized with OVA plus CT or acridinium-labeled CT, comparable levels of OVA-specific Ab responses were noted (data not shown).

2.7. Determination of IgE Abs

Total IgE Abs titers in plasma were determined using a sandwich ELISA [23]. Plasma samples were collected 1 week after the last immunization. Concentrations of total IgE Abs in plasma were calculated using a standard curve. OVA-specific IgE Abs responses were determined by an IgE capture method [15,16]. TMB+ (3,3′,5,5′,-tetramethylbenzidine; DAKO, Carpinteria, CA) were used as substrate-chromogen. Endpoint titers were expressed as the reciprocal $\log_2$ of the last dilution that gave an optical density at 450 nm (OD_{450}) of ≥0.1 OD unit above the OD_{450} of negative controls after a 15-min incubation. Incubations were terminated by addition of 0.5 M H_2SO_4.

2.8. Detection of OVA or CT-B-specific Abs

One week after the last immunization, blood and mucosal secretions (fecal extracts, saliva, nasal washes, and vaginal washes) were collected. The collecting methods used have been previously described elsewhere [32,36,37]. Titers of OVA-specific or CT-B-specific Ab in samples were determined by an endpoint ELISA [36]. For each experiment, vaginal washes were pooled from four mice. Endpoint titers were expressed as the reciprocal $\log_2$ of the last dilution that gave an OD at 450 nm (OD_{450}) of ≥0.1 OD unit above the OD_{450} of negative controls after a 15-min incubation.

2.9. Detection of OVA-specific Ab-forming cells (AFCs)

Single-cell suspensions were obtained from NALT, nasal lamina propria (n-LP), small intestinal lamina propria (i-LP), mesenteric lymph nodes (MLNs), submandibular lymph nodes (SMLNs), submandibular glands (SMGs), spleen and axially lymph nodes (ALNs) were prepared as described elsewhere [30,36,37]. OVA-specific IgG and IgA AFCs in the mucosal and systemic tissues of mice were determined by ELISPOT assay [3,23]. The numbers of OVA-specific AFCs were quantitated with the aid of a stereomicroscope.

2.10. GM1-binding assay

Nunc immunoplates were coated with a ganglioside GM1. Specified concentrations of APE and CT (final concentration: 10 ng/ml) were mixed well and added into each well after blocking with 1% BSA. To detect GM1 binding by CT, we used mouse anti-CT serum at a dilution of 1:1000, followed by horseradish peroxidase-conjugated goat anti-mouse IgG (H + L) Abs. The plates were developed at room temperature with TMB+ substrate-chromogen. Incubations were terminated by addition of 0.5 M H_2SO_4, and optical density was measured at 450 nm.

2.11. Statistics

The results are expressed as the mean ± the standard error of mean (SEM). Normally distributed variables were compared by the two-tailed Student's *t* test and nonnormally distributed variables by the two-tailed Mann–Whitney *U* test. A *p* value of <0.05 was considered significant.

3. Results

3.1. APE reduced toxicity of CT in vitro

If the toxicity of CT could be mitigated or eliminated by the use of APE, its efficacy as a mucosal adjuvant could be fully harnessed in humans. To assess the ability of APE to reduce CT toxicity, we initially performed a Y-1 adrenal cell assay and determining ECi. When CT was added into the Y-1 cell cultures together with varying concentrations of APE, the toxicity of CT was reduced in a dose-dependent manner (Fig. 1A). At a molar rate of 1:1000 and 1:100 of CT and APE, a combination of CT/APE had 1/731 and 1/17 fewer toxic activities for ECi, respectively, than did CT alone. Since the morphological response of cells to CT has been shown to be dependent upon adenylcyclase-mediated increases in cAMP [38], we next assessed the induction of cAMP by CT with or without APE. When more than 10 μg/ml (1:100 to 1:1000) of APE was administered, cAMP levels were significantly decreased (Fig. 1B). APE alone did not change cAMP levels in controls. These results demonstrate that APE reduced the ADP-ribosyltransferase activity of CT *in vitro*.

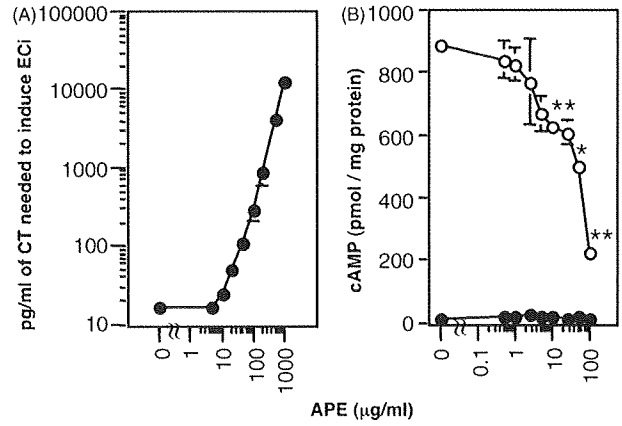

Fig. 1. Morphological responses of Y-1 cells and cAMP induction in CHO cells by CT with or without APE. (A) Morphological changes of Y-1 cells were assessed by culture with CT and several concentrations of APE. The data show the concentration of CT initiating rounding of Y-1 cells as ECi. The data for ECi are shown as the mean concentration ± one SEM for three different experiments. (B) CHO cells were cultured with specified concentrations of APE alone (closed circle) or together with 100 ng/ml of CT (open circle). The levels of cAMP were expressed as pmol of cAMP/mg of protein. The data for cAMP induction are shown as the mean level ± one SEM for three different experiments. Significant differences between the CT-only group and the CT plus APE group are indicated by asterisks (*$p < 0.05$, **$p < 0.005$).

3.2. APE reduced inflammatory responses induced by CT in vivo

Histopathologic studies allowed us to compare the inflammatory responses in the nasal cavity of mice given nasal OVA plus CT with one of several specified dosages of APE and without APE. The severity of the inflammatory response was scored as described in Section 2, and representative histopathology images of each grade are shown in Fig. 2A. In all four mice nasally immunized with OVA and 0.5 μg of CT without APE, grade 3 or 4 inflammatory responses (with an inflammatory layer ≥10 cells thick) were observed (Fig. 2B). However, inflammatory responses were reduced in mice given nasal OVA plus 0.5 μg of CT in the presence of 50–500 μg (1:100 to 1:1000) of APE. Indeed, grade 1 inflammatory responses (inflammatory layer <5 cells thick) were observed in two of the four mice given 500 μg (1:1000) of APE (Fig. 2B).

Since it has been shown that nasal CT redirected co-administrating tetanus toxoid into the ON/E and NALT within 3 h, with highest levels of IL-1β and IL-6 expression over the next 3 h [39], we next assessed IL-1β, IL-6, and TNF-α productions in nasal washes after 6 h of administration of vaccines in order to detect early inflammatory responses. The mean level of IL-6 in nasal washes of mice nasally immunized with OVA plus CT without APE was 601.9 ± 35.7 pg/ml. As a reference, the level of IL-6 in nasal washes of mice administered PBS alone was 13.9 ± 4.6 pg/ml. The

IL-6 levels in nasal washes of mice given nasal OVA and 0.5 μg of CT together with 100–500 μg (1:200 to 1:1000) of APE were significantly lower than in mice immunized with OVA plus CT. Tenfold lower levels of IL-6 were observed in mice immunized with OVA and CT together with 500 μg of APE when compared with mice nasally immunized with OVA and CT alone (Fig. 2C). In contrast, essentially no IL-1β or TNF-α was detected in nasal washes (data not shown).

Furthermore, real-time RT-PCR was performed to quantify levels of inflammatory cytokine-specific mRNA expression in nasal tissues and brains. The levels of IL-1β-, IL-6-, and TNF-α-specific mRNA were significantly higher in the palates, including the NALT and nasal septums with nasal mucosa of mice administrated OVA plus CT than negative control mice. Though IL-1β and TNF-α were not detected in nasal wash samples by ELISA, levels of IL-1β-, IL-6-, and TNF-α-specific mRNA expression in nasal tissues of mice administrated OVA plus CT with 100 or 500 μg of APE were significantly decreased when compared with mice given CT without APE. In particular, the palates and nasal septums of mice with 500 μg of APE exhibited significantly low level of IL-6-specific mRNA expression (a decrease of 83%, $p = 0.0003$, and 94%, $p = 0.002$, respectively) (Fig. 2D). In contrast, no significant changes in inflammatory cytokine-specific mRNA levels in OBs, frontal regions and basal ganglia regions were noted (data not shown).

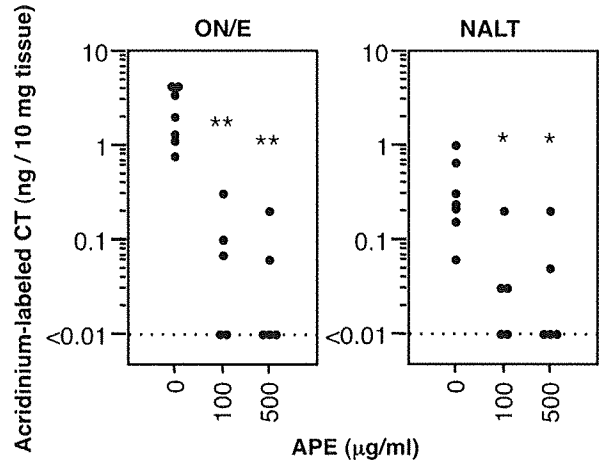

Fig. 3. Comparison of the distribution of CT in olfactory tissues of mice immunized with OVA plus CT with or without nasal APE. Distribution of acridinium-labeled CT into the NALT and ON/E was determined 6 h after nasal administration of 0.5 μg of CT with 0, 100 or 500 μg of APE. The NALT and ON/E were collected and analyzed for presence of acridinium-labeled CT. Data are expressed as ng of CT/10 mg weight of tissue. The CNS tissues of mice given nasal PBS were examined for background levels of luminescent. These control values were subtracted from each experimental value. Significant differences between the CT-only group and the CT plus APE group are indicated by asterisks (*$p < 0.05$, **$p < 0.005$).

3.3. *APE reduced accumulation of CT in the nasal and CNS tissues*

Our studies showed that APE reduced inflammatory responses and inflammatory cytokines production by CT in the nasal tissues. Though the biological and pathogenic consequences of CT in the CNS is not understood, it is most important to confirm CNS toxicity for the safety of this nasal vaccine. CT accumulation levels were significantly lower in NALT and ON/E of mice nasally immunized with OVA plus 0.5 μg of acridinium-labeled CT together with 100 and 500 μg (1:200 and 1:1000) of APE than in mice immunized with OVA plus CT after 6 h (Fig. 3). In contrast, the acridinium-labeled CT in OBs was very low or undetectable (<0.02 ng/10 mg tissue) and there were no significant changes in groups immunized with or without APE (data not shown). These results clearly show that CT

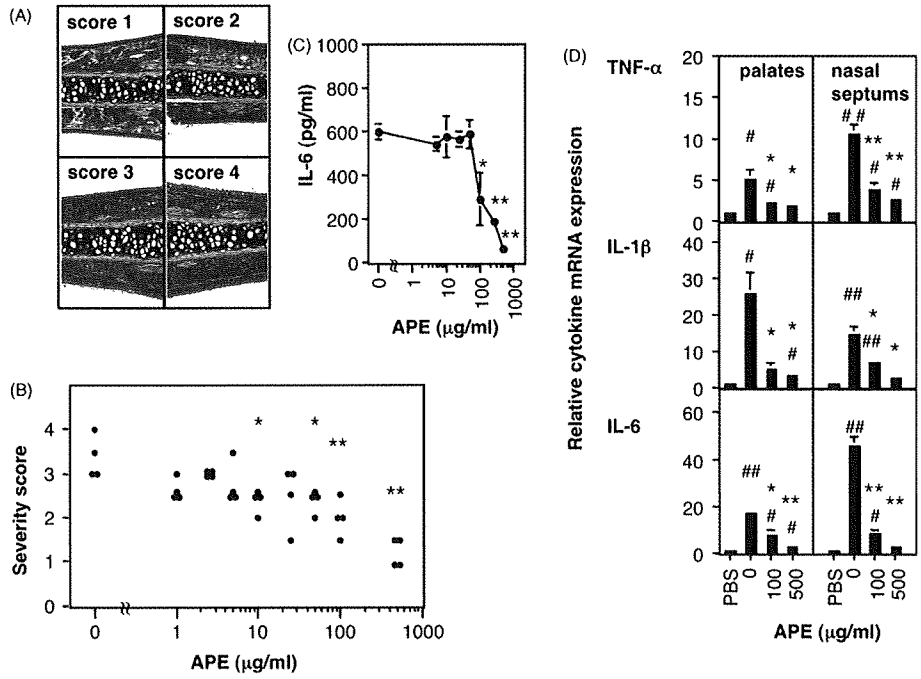

Fig. 2. Inflammatory responses in the nasal cavity of mice nasally immunized with OVA plus CT with or without APE. (A) Frontal cross-sections of the nasal cavity of mice were taken at 1 week after the last immunization. The severity of the lesions in each mouse was scored on a 1–4 grade based on the thickness of the inflammatory cell layer. Representative histopathology images of each grade are shown. (B) Inflammation was graded in the first two slices from the nasal apex of each mouse, and a mean calculated to determine the inflammatory score for each mouse. (C) The concentrations of IL-6 in the nasal washes of mice immunized with OVA plus CT with or without APE were determined by IL-6-specific ELISA. The data are shown as the mean level ± one SEM for 12 mice in each experimental group, and the data are representative of three separate experiments. (D) Real-time quantitative RT-PCR analysis was performed to compare cytokine-specific mRNA expression in the nasal tissues. Results are presented as fold decrease or increase compared with mice administered PBS alone. The data are shown as the mean level ± one SEM for 4 mice in each experimental group and the data are representative of two separate experiments. Significant differences between the CT-only group and CT plus APE group are indicated by asterisks (*$p < 0.05$, **$p < 0.005$), and the PBS alone group and CT plus APE group are indicated by squares ($^{\#}p < 0.05$, $^{\#\#}p < 0.005$).

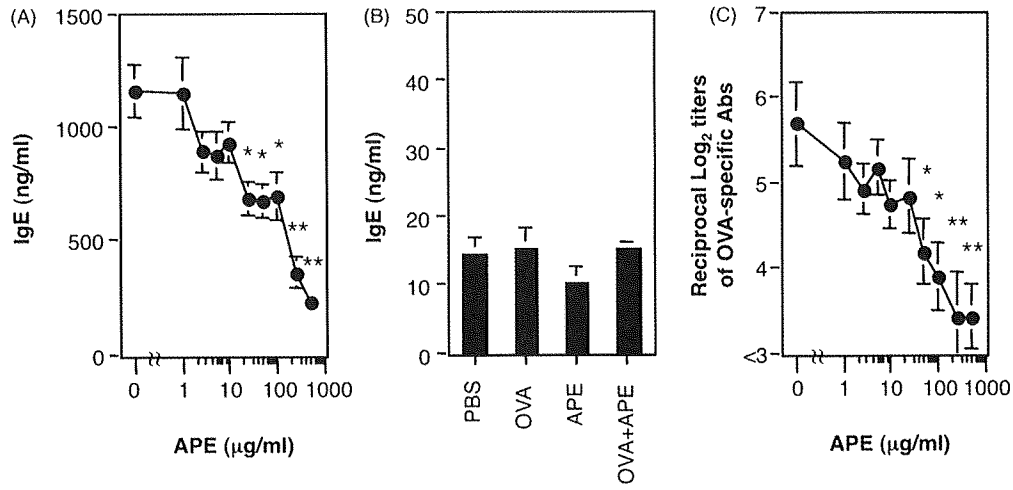

Fig. 4. Total and OVA-specific IgE Ab responses in plasma of mice given nasal OVA plus CT with or without APE. Mice were nasally immunized with OVA plus CT with different doses of APE three times weekly intervals. Plasma samples were collected 1 week after the last nasal immunization. (A) The levels of total IgE Abs were determined by sandwich ELISA. (B) As reference data, the levels of total IgE Abs in the plasma of mice administered PBS alone, 100 μg of OVA, 500 μg of APE, or 100 μg of OVA plus 500 μg of APE were determined. (C) The titers of OVA-specific IgE Abs in the plasma of mice co-administered different doses of APE were determined by OVA-specific IgE ELISA. The data are shown as the mean concentration ± one SEM for 12 mice in each experimental group, and the data are representative of three separate experiments. Significant differences between the CT-only group and the CT plus APE group are indicated by asterisks (*$p < 0.05$, **$p < 0.005$).

fails to accumulate in the ON/E in the presence of the optimal dose of APE.

3.4. APE reduced total and OVA-specific IgE Ab responses

In addition to its toxicity, one of the drawbacks of CT is the induction of high IgE Ab responses to bystander Ags. To determine whether the combination of APE and CT down-regulates IgE Ab responses, we assessed total IgE Abs in the plasma of mice nasally immunized with OVA plus CT with or without APE. Significantly lower level of total IgE Ab responses were seen in the plasma of mice given 25–500 μg (1:50 to 1:1000) of nasal APE than in those without APE (Fig. 4A). The control groups of mice given nasal PBS, OVA alone, 500 μg of APE, or OVA plus 500 μg of APE, resulted in identical low total IgE Ab titers (Fig. 4B). We next assessed OVA-Specific IgE Abs in the plasma of mice nasally immunized with OVA plus CT with or without APE by endpoint ELISA. Significant reductions in OVA-specific IgE Ab titers were observed in the plasma of mice given nasal OVA plus 0.5 μg of CT together with 50–500 μg (1:100 to 1:1000) of APE (Fig. 4C).

3.5. APE maintained induction of OVA-specific IgA Abs in mucosal secretions

It is important to show co-administration of APE does not affect the adjuvanticity of nasal CT. In this regard, mice were nasally immunized with OVA plus CT alone or together with one of several specified dosages of APE. One week after the last immunization the levels of OVA-specific IgA Abs in mucosal secretions (fecal extracts, nasal washes, saliva and vaginal washes) were examined by end-point ELISA. Mice nasally immunized with OVA plus 0.5 μg of CT together with 1–250 μg (1:2 to 1:500) of APE showed OVA-specific IgA Abs in mucosal secretions that were essentially identical to those observed in mice immunized with OVA plus CT alone (Fig. 5). In contrast, mice given nasal OVA plus 0.5 μg of CT together with 500 μg (1:1000) of APE revealed significantly reduced titers of OVA-

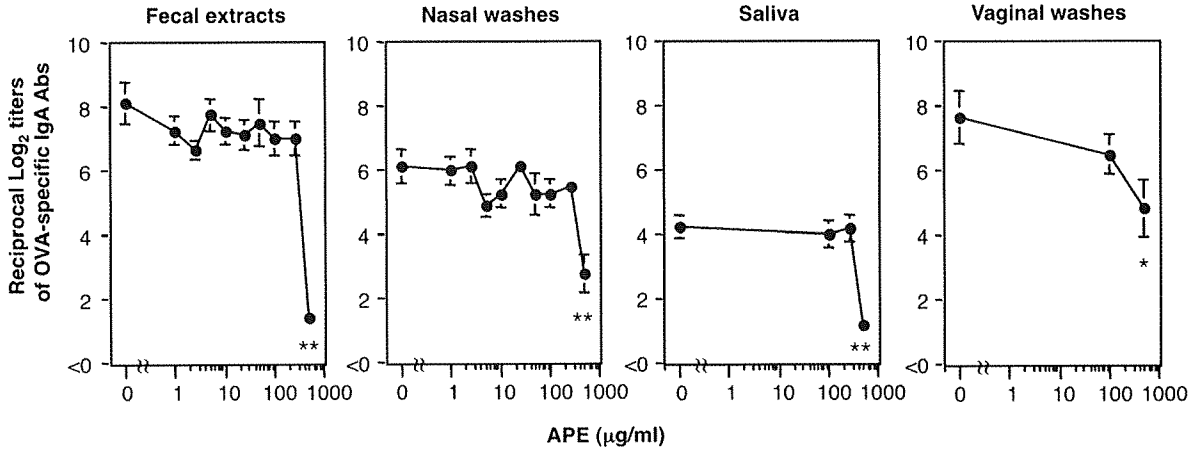

Fig. 5. OVA-specific IgA Ab responses in mucosal secretions of mice nasally immunized with OVA plus CT with or without nasal APE. Mice were nasally immunized with OVA plus CT with different doses of APE three times weekly intervals. Mucosal secretions (fecal extracts, nasal washes, saliva, and vaginal washes) were collected 1 week after the last immunization. OVA-specific IgA Ab levels in the mucosal secretions were determined by OVA-specific endpoint ELISA. The data for fecal extracts, nasal washes, and saliva are shown as the mean titer ± one SEM for 12 mice in each experimental group, and the data are representative of three separate experiments. The samples of vaginal washes were pooled from four mice, and six pooled samples were assessed by ELISA. Significant differences between the CT-only group and CT plus APE group are indicated by asterisks (*$p < 0.05$, **$p < 0.005$).

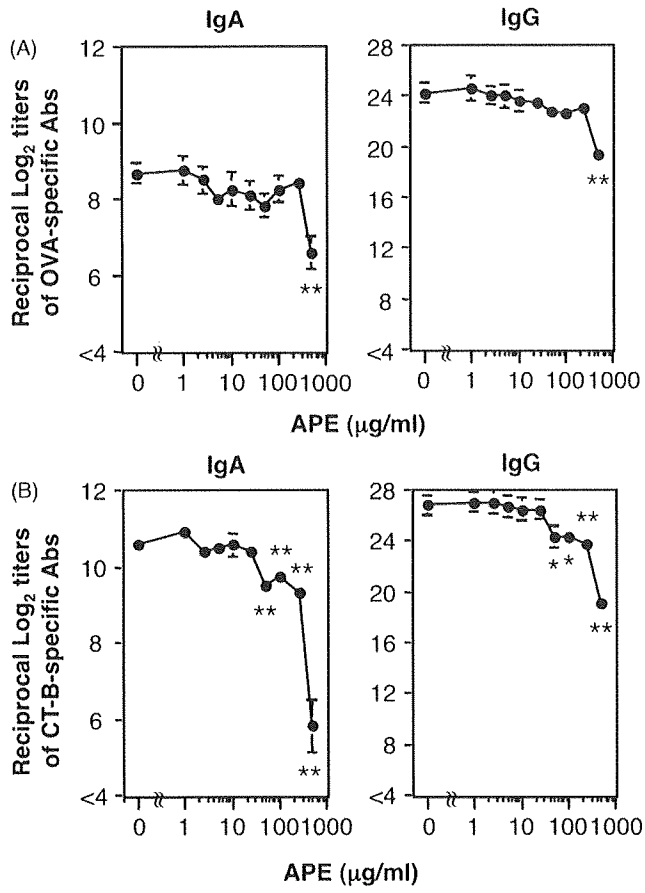

Fig. 6. OVA- or CT-B-specific IgA and IgG Ab responses in the plasma of mice immunized with OVA plus CT with or without nasal APE. Mice were immunized as described in Fig. 5 legend and plasma samples of each group of mice were collected 1 week after the last nasal immunization. The titers of OVA- (A) or CT-B- (B) specific IgA and IgG Abs in the plasma were determined by OVA- or CT-B-specific endpoint ELISA. The data are shown as the mean titer ± one SEM for 12 mice in each experimental group and the data are representative of three separate experiments. Significant differences between the CT-only group and the CT plus APE group are indicated by asterisks ($^{*}p < 0.05$, $^{**}p < 0.005$).

specific IgA Abs in mucosal secretions (Fig. 5). These results suggest that APE dosages of less than 500 μg (1:1000) could maintain the mucosal adjuvant ability of CT to induce Ag-specific IgA Abs in mucosal secretions.

3.6. APE maintained OVA-specific IgA and IgG Abs in plasma

We next analyzed systemic immune responses. The plasma of mice nasally immunized with OVA plus CT alone or with one of several specified dosages of APE were subjected to endpoint ELISA in order to assess the levels of OVA-specific IgA and IgG Abs. Similar levels of OVA-specific IgA and IgG Ab responses were detected in plasma of mice given 0–250 μg (up to 1:500) of APE (Fig. 6A); however, these OVA-specific Ab titers were significantly reduced when 500 μg (1:1000) of APE was employed. Identically, the dose-dependent APE effect was also noted for OVA-specific IgA Ab responses in mucosal secretions (Fig. 5). When CT-B-specific IgA and IgG Ab responses were examined, significantly reduced titers were observed in the plasma of mice nasally immunized with OVA plus 0.5 μg of CT together with 50–500 μg (1:100 to 1:1000) of APE. These results suggest that lower doses of APE could alter antigenicity of CT when compared with APE doses which influence CT adjuvanticity (Fig. 6B).

3.7. Comparison of OVA-specific Abs subclass IgG in plasma

We next investigate OVA-specific IgG subclass Ab responses in plasma of mice nasally immunized with OVA plus CT with or without APE. In all groups of mice, OVA-specific IgG1 Ab levels were highest, followed by Ab subclasses of IgG2b, IgG2a, and IgG3 (Fig. 7). As we anticipated, 500 μg (1:1000) of APE significantly reduced OVA-specific IgG1, IgG2a, IgG2b and IgG3 Ab titers in the plasma; however, co-administration of 1–250 μg (1:2 to 1:500) of APE showed intact IgG subclass responses (Fig. 7). When we calculated the ratio of IgG1 to IgG2a titers for each mouse, the mean values of the ratio were essentially unchanged regardless APE dosage (data not shown).

3.8. Assessment of OVA-specific AFCs in the mucosal and systemic tissues

In order to confirm OVA-specific Ab responses at the cellular level, we next compared the number of OVA-specific AFCs in the mucosal (NALT, n-LP, i-LP, MLNs, SMLNs and SMGs) and systemic (spleen and ALNs) lymphoid tissues 1 week after last nasal immunization with OVA plus 0.5 μg of CT with 0 μg (1:0), 100 μg (1:200), or 500 μg (1:1000) of APE. Significantly reduced number of OVA-specific IgA and IgG AFCs were seen in the n-LP, i-LP, SMLNs, SMGs and spleen of mice co-administered of 500 μg (1:1000) of APE (Fig. 8).

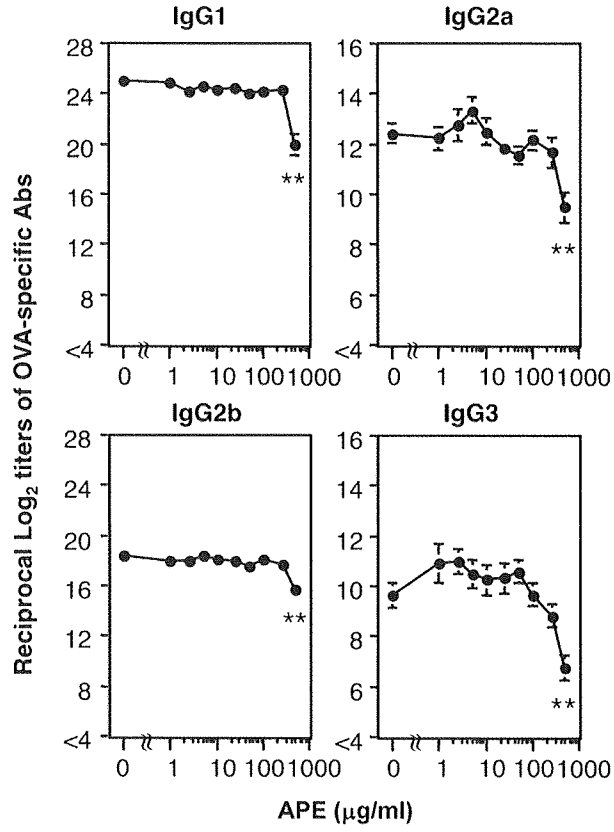

Fig. 7. OVA-specific IgG subclass Ab responses in the plasma of mice nasally immunized with OVA plus CT with or without nasal APE. Mice were immunized as described in Fig. 5 legend and plasma samples of each group of mice were collected 1 week after the last nasal immunization. The titers of OVA-specific IgG1, IgG2a, IgG2b, and IgG3 Abs in the plasma were determined by OVA-specific endpoint ELISA. The data are shown as the mean titer ± one SEM for 12 mice in each experimental group and the data are representative of three separate experiments. Significant differences between the CT-only group and the CT plus APE group are indicated by asterisks ($^{**}p < 0.005$).